Crystallographic and Biochemical Investigation of the Lead(II)-Catalyzed Hydrolysis of Yeast Phenylalanine tRNA

R. S. Brown,‡ J. C. Dewan,§ and A. Klug*

MRC Laboratory of Molecular Biology, Hills Road, Cambridge CB2 2QH, England

Received July 5, 1984; Revised Manuscript Received December 12, 1984

ABSTRACT: X-ray diffraction data from monoclinic crystals of yeast $tRNA^{Phe}$ soaked in dilute lead(II) acetate solutions at pH 5.0 and at pH 7.4 have been collected to a resolution of 3 Å, and the Pb(II) binding sites have been obtained by difference Fourier analyses. The same three Pb(II) binding sites are observed at both of these pH values. At pH 7.4 an extra peak of negative electron density appears on the difference map close to one of the Pb(II) binding sites and at the position of phosphate-18, indicating cleavage of the sugar–phosphate chain between residues D-17 and G-18 of the $tRNA^{Phe}$ molecule in this derivative. Chain scission does not occur to any observable extent in the structure at pH 5.0, and we have, therefore, a picture of the reactants (at pH 5.0) and products (at pH 7.4) of this cleavage reaction. Polyacrylamide gel electrophoresis as well as sequencing experiments confirms the cleavage of the $tRNA^{Phe}$ molecule into one-fourth and three-fourth fragments, with the shorter fragment consisting essentially of residues G-1 through D-17 while the larger fragment contains residues G-18 through A-76. End-group analyses suggest a ribose cyclic 2′,3′-phosphate at D-17 of the one-fourth fragment with a 5′-OH at G-18 of the three-fourth fragment. Cleavage of the $tRNA^{Phe}$ molecule does not occur in the absence of Pb(II), and the proximity of one of these metal ions to the cleavage site strongly implicates this metal ion in the cleavage reaction. Consideration of several possible mechanisms for the reaction, taking into account the biochemical and crystallographic facts presented above, suggests that the cleavage involves removal of the proton from the 2′-OH of ribose-17 by a Pb(II)-bound hydroxyl group. Subsequent nucleophilic attack of the resulting 2′-O^- on the phosphorus atom of phosphate-18, presumably through a pentacoordinate phosphorus cyclic intermediate (as in the action of pancreatic ribonuclease A), results in chain scission. It cannot be decided whether the displacement, within the pentacoordinate intermediate, proceeds via an *in-line* or *adjacent* pathway, but an exploration of the likelihood of either pathway is presented. Strand cleavage at the particular site occurs fortuitously because the aquo Pb(II) ion binds at the correct distance and presumably in such a manner as to present a hydroxyl group in the correct orientation to effect the proton abstraction. The pK_1 of a Pb(II)-bound water molecule is approximately 7, which will facilitate reaction at that pH but will slow it substantially at pH 5.0. The crystallographic experiments indicate that the occupancy of the Pb(II) ion involved in the cleavage reaction is reduced by approximately 50% in the structure at pH 7.4 compared with that at pH 5.0. We conclude from this that the cleavage reaction may well be catalytic, rather than stoichiometric, since Pb(II) would be released after cleavage has occurred and may then be able to effect further cleavages. This is corroborated by biochemical experiments. The implications of this work for the toxicity of lead are examined.

RNA is inherently rather unstable, owing to the presence of the 2′-OH group located on each ribose ring, and is degraded under mildly basic and acidic conditions as well as by the action of certain metal ions (Brown & Todd, 1952; Brown, 1974; Eichhorn, 1975). DNA, on the other hand, where this hydroxyl group is replaced by a proton, is quite resistant to attack, and indeed, it has been suggested that it is this stability that has led to DNA being selected as the primary genetic material rather than RNA (Butzow & Eichhorn, 1975). A large body of work has been published concerning the degradation of RNA by metal ions (Dimroth et al., 1950, 1959; Bamann et al., 1954; Dimroth & Witzel, 1959; Witzel, 1959; Huff et al., 1964; Trapmann & Devani, 1965), and a certain amount of this work has been specifically concerned with the action of Pb(II) (Britten, 1962; Farkas, 1968, 1975; Farkas et al., 1972). Metal ion degradation has also been performed on various synthetic polyribonucleotides in an attempt to gain insight into the mechanisms of these reactions and to identify any sequence specificity that may be operative (Eichhorn & Butzow, 1965; Butzow & Eichhorn, 1965, 1971; Eichhorn et al., 1967, 1971), and work on various tRNAs shows that site-specific cleavages can be brought about in these macromolecules by the action of Mg(II) and Pb(II) (Wintermeyer & Zachau, 1973; Werner et al., 1976). Of all the metal ions that have been reacted with RNA, it is Pb(II) that will depolymerize the molecule most rapidly, with Zn(II) being next best (Farkas, 1968, 1975).

The crystal structure of the monoclinic modification of $tRNA^{Phe}$ was elucidated nearly a decade ago (Ladner et al., 1972, 1975; Robertus et al., 1974; Jack et al., 1976; Hingerty et al., 1978). During the period when suitable heavy-atom derivatives were being sought, for use in the isomorphous

‡Recipient of an EMBO short-term fellowship. Present address: European Molecular Biology Laboratory, D-6900 Heidelberg, West Germany.

§Thomas C. Usher Fellow, 1981–1982. Present address: Department of Chemistry, Massachusetts Institute of Technology, Cambridge, MA 02139.

0006-2960/85/0424-4785$01.50/0

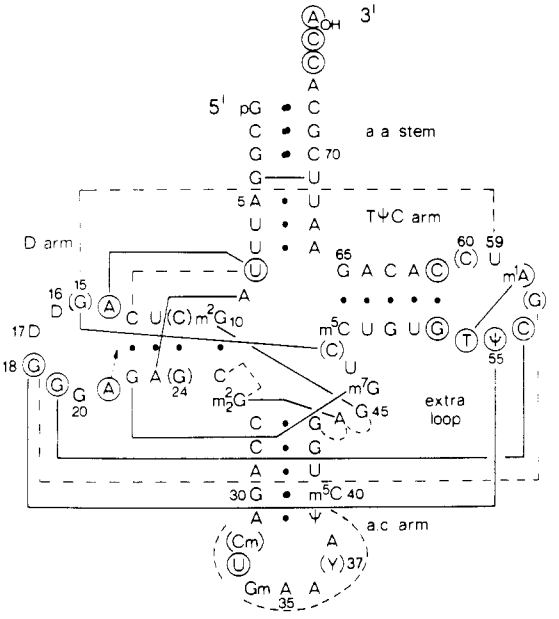

FIGURE 1: Nucleotide sequence of yeast $tRNA^{Phe}$ arranged in the cloverleaf formula. Bases that are invariant in all tRNA sequences are circled while semiinvariants, that is, purines or pyrimidines, exclusively appear in parentheses. Solid circles represent Watson–Crick base pairing while other pairs of hydrogen-bonded bases are joined by solid lines. Bases, apart from those in Watson–Crick double-helical regions, that stack on one another in the tertiary structure are joined by dashed lines. Hydrogen bonding by A-21 to riboses-8 and -48 is indicated by a dashed arrow. The three Pb(II) ion binding sites are as follows: Pb(1) binds at U-59 and C-60, Pb(2) at G-45, and Pb(3) at Y-37.

replacement method, $Pb(OAc)_2$[1] was tested as a possible candidate. Before the $tRNA^{Phe}$ structure was eventually solved, it was already known that $Pb(OAc)_2$ did give a derivative that was isomorphous with the native structure, but a difference Patterson map could not be solved for the Pb(II) positions. Once the $tRNA^{Phe}$ structure had been solved, however, the location of metal ions in any isomorphous derivative becomes a fairly easy task by simply computing a difference Fourier map between native and derivative structures (Jack et al., 1977; Hingerty et al., 1982). When this was done for the Pb(II) derivative, three peaks of positive electron density on the difference Fourier map, corresponding to three Pb(II) ions bound to the $tRNA^{Phe}$ molecule (Figure 1), were observed as well as an unexpected large peak of negative electron density that was located at the position of what was a phosphate group in the native structure (Figure 2a). Whereas a positive peak signifies a feature present in the derivative that is absent in the native, a negative peak signifies the opposite situation and in the present case suggested that chain scission had occurred in the derivative since the phosphate group appeared to have either moved or been lost. Furthermore, the negative peak is close to one of the three bound Pb(II) ions (Figure 2a), and previous work by Werner et al. (1976) had shown that Pb(II) would give a site-specific cleavage in this region of the $tRNA^{Phe}$ molecule, thus strongly implicating this Pb(II) ion in the cleavage reaction.

There are essentially two catalytic mechanisms by which a metal ion can bring about a reaction in a macromolecule (Fersht, 1977). One is by an electrophilic activation mechanism, which is essentially pH independent, and the other is by the production of hydroxyl ions at or near neutral pH, which is a pH-dependent process. Our crystallographic results, performed at pH 7.4, suggested that we were looking at the tRNA after strand cleavage had occurred, and careful consideration of various factors suggested that the pH-dependent process was operative. We could not, however, tell whether the Pb(II) ion near the cleavage site represented a position to which Pb(II) had moved after cleavage or whether it also represented the Pb(II) position before cleavage. A preliminary biochemical experiment was performed on the tRNA with added Pb(II) at pH 5.0 and pH 7.4. We surmized that if the reaction was pH dependent, it should be slowed substantially at pH 5.0, since the pK_1 for aquo Pb(II) is ca. 7 and the concentration of the $(Pb–OH)^+$ species should be minimal at the lower pH. The experiment confirmed that strand cleavage was very slow at pH 5.0 and was quite rapid at pH 7.4. We were already in possession of X-ray data collected on the Pb(II) derivative at pH 7.4, where significant strand cleavage had occurred, and we were then able to collect data at pH 5.0 before any observable amount of such cleavage could have occurred. We have, therefore, a stereochemical picture of the situation before (at pH 5.0) and after (at pH 7.4) cleavage, and we have been able to examine possible mechanisms for the observed strand scission.

A preliminary account of the work presented here has been published (Brown et al., 1983). Similar Pb(II) binding sites, as well as the strand scission, have subsequently also been reported in crystals of the orthorhombic modification of $tRNA^{Phe}$ at pH 6.5 (Rubin & Sundaralingam, 1983). In this paper we present a detailed account of the biochemical experiments, carried out in parallel with the crystallographic study, but not so far described. A detailed discussion of various other points that could only be given cursory treatment in the preliminary account is also given.

Materials and Methods

Preparation of Crystals. Monoclinic crystals of brewers' yeast $tRNA^{Phe}$ (Boehringer-Mannheim) were grown by the dialysis method (Ladner et al., 1972) except that the buffer was 10 mM Tris-HCl, pH 7.4, and the precipitant was 6% (w/v) hexane-1,6-diol (BDH). After crystallization the dialyzate was changed to 15 mM $MgCl_2$, 1.5 mM spermine tetrahydrochloride, 20% (w/v) hexane-1,6-diol, and either 10 mM potassium acetate, pH 5.0, or 10 mM Tris-HCl, pH 7.4.

Pb(II) Cleavage Reaction. A 50-mL stock solution of 10 mM $Pb(OAc)_2$ was prepared with the addition of 1 drop of glacial acetic acid. The effects of pH, Pb(II) concentration, temperature, and reaction time were investigated. Crystals were soaked in 1 mM $Pb(OAc)_2$ and removed at intervals over a period of several weeks at 4 °C to follow the reaction time course. Pb(II) cleavage in solution at pH 5.0, 7.4, and 9.0 was performed with 20 μM $tRNA^{Phe}$ at room temperature in mother liquor from which the hexane-1,6-diol was omitted.

Gel Electrophoresis. Analysis of the cleavage products of $tRNA^{Phe}$ was by electrophoresis in an 18% polyacrylamide–7 M urea slab gel (20 cm × 15 cm × 0.15 cm). The gel was polymerized from 18% (w/v) acrylamide, 0.9% (w/v) bis(acrylamide), 7 M urea, 90 mM Tris–borate (pH 8.3), and 2.5 mM Na_2EDTA. Crystals were isolated from mother liquor, dissolved in 8 M urea, 40 mM EDTA, pH 7.0, and 0.025% bromophenol blue, and heated for 1 min at 95 °C. Electrophoresis was for 24 h at 100 V. RNA bands were visualized with ultraviolet light after staining with ethidium bromide (2 mg/L).

[1] Abbreviations: EDTA, ethylenediaminetetraacetic acid; EGTA, ethylene glycol bis(β-aminoethyl ether)-*N,N,N',N'*-tetraacetic acid; HMHD, (hydroxymercuri)hydroquinone *O,O*-diacetate; OAc, acetate; RNase A, bovine pancreatic ribonuclease A; tbp, trigonal bipyramid; Tris-HCl, tris(hydroxymethyl)aminomethane hydrochloride.

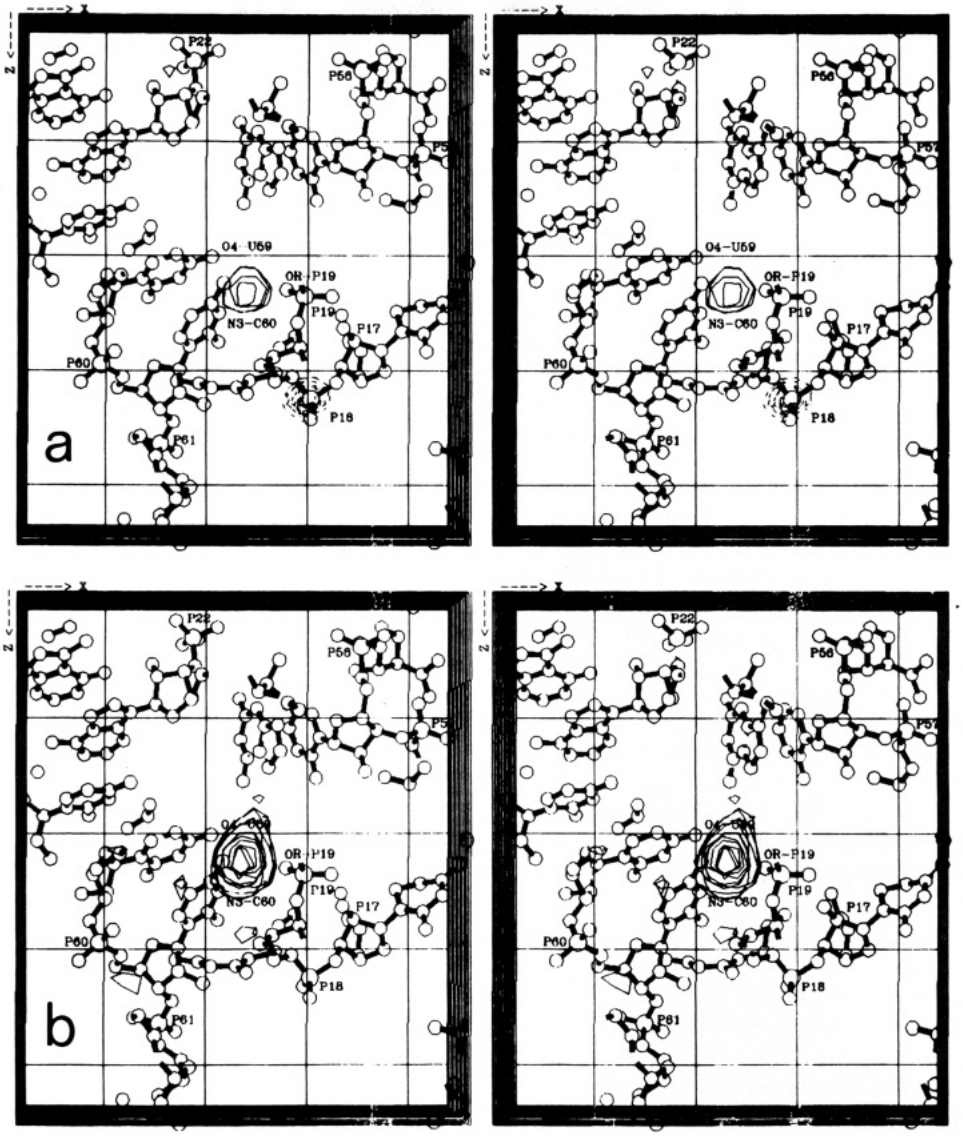

FIGURE 2: Stereoviews of the $|F_{Pb}| - |F_{native}|$ difference Fourier maps of yeast tRNA^{Phe} in a slab 8 Å thick centered on the Pb(II) ion at the Pb(1) cleavage site: (a) pH 7.4, (b) pH 5.0. The refined native structure is superimposed, and each phosphorus atom is labeled. Both derivative structures were scaled to the native structure, and the same contour levels have been used in (a) and (b). The large positive peaks (unbroken lines) correspond to the Pb(II) ion at site Pb(1) while the large negative peak (broken lines) in (a), centered on phosphate-18, represents sugar–phosphate backbone cleavage between residues D-17 and G-18 at pH 7.4. The Pb(II) ion is bound directly to O4(U-59) and N3(C-60) with a long contact to OR(P-19).

Isolation of tRNA^{Phe} Fragments. Crystals were soaked for 3 weeks in 1 mM $Pb(OAc)_2$ (pH 7.4) at 4 °C, separated from mother liquor, and subjected to 15% polyacrylamide–7 M urea preparative gel electrophoresis. Gel slices containing RNA were crushed and soaked overnight in 0.5 M NaOAc, 10 mM EDTA, and 100 mM Tris-HCl, pH 7.5. The eluates were passed through Millex 0.45-μm filter units (Millipore Corp.) and collected in siliconized 15-mL Corex tubes (Sorvall). RNA was precipitated with 3 volumes of 95% ethanol at −20 °C. The pellets were collected by centrifugation at 12000*g* for 30 min, and residual NaOAc was removed by repeated ethanol precipitation.

Location of the Cleavage Site. A 1-μg sample of the three-fourth fragment of tRNA^{Phe} was phosphorylated at the 5′-terminus with [γ-^{32}P]ATP (Amersham) and T4 polynucleotide kinase (Walker & RajBhandary, 1975). The reaction mixture was applied together with 1 A_{260} unit of carrier tRNA^{Phe} onto a DEAE-cellulose (0.5 cm × 0.5 cm) column equilibrated with 50 mM Tris-HCl, pH 8.0–1 mM EDTA. Nonincorporated radioactivity was eluted with 0.4 M KOAc. The retained 5′-^{32}P end-labeled fragment was eluted with 1 M KOAc and recovered by precipitation with ethanol. A partial digest of the 5′-^{32}P end-labeled fragment was obtained with nuclease P1 (Boehringer-Mannheim) in 50 mM ammonium acetate, pH 5.3. The digestion products were separated by two-dimensional homochromatography using a 3% homomix (Silberklang et al., 1979) and located by autoradiography. Prefogged Fuji RX X-ray film and a Du Pont Lightning-Plus intensifying screen were employed at −70 °C to hasten autoradiography of ^{32}P.

5′ End Group at Cleavage Site. The 5′-^{32}P end-labeled fragment was digested exhaustively with nuclease P1. The digest was applied to a cellulose (20 cm × 20 cm) thin-layer plate (Merck) and chromatographed in parallel with nonradioactive nucleotide 5′-monophosphate markers (Sigma Chemicals) in solvent system A, isobutyric acid–NH_4OH–H_2O (66:1:33) (Nishimura, 1972). The 5′-^{32}P-labeled nucleotide was located by autoradiography and identified by comparison with standards visualized with ultraviolet light.

Demonstration of Cyclic 2′,3′-Phosphate. The presence of a cyclic 2′,3′-phosphate at the 3′-terminus of the one-fourth tRNA^{Phe} fragment was investigated by enzymatic 3′-^{32}P end

labeling before and after the following treatments: (1) incubation in 20 mM Tris-HCl, pH 8.0, with calf intestinal alkaline phosphatase (Boehringer-Mannheim) for 1 h at 37 °C to remove terminal phosphate; (2) treatment with 0.1 M HCl for 1 h at room temperature to convert cyclic 2′,3′-phosphate to 3′-monophosphate (Markham & Smith, 1952); (3) 0.1 M HCl treatment, neutralization, followed by phosphatase to produce a free terminal 3′-OH group. Inactivation of phosphatase was by addition of 5 mM EGTA, pH 7.9, and boiling for 4 min (Silberklang et al., 1977).

3′-^{32}P end labeling was accomplished with T4 RNA ligase (New England Bio-Labs) and [5′-^{32}P]pCp (Amersham) under conditions that worked successfully for intact tRNA^{Phe} (England et al., 1980). After incubation for 12 h at 8 °C, the 3′-^{32}P-labeled fragment was purified from smaller breakdown products by preparative 15% polyacrylamide gel electrophoresis, located by autoradiography, excised, and recovered as described below. Radioactivity was determined by Cerenkov counting in a Beckman LS8100 scintillation spectrometer.

3′ End Group at Cleavage Site. Complete digestion of the 3′-^{32}P end-labeled fragment was achieved by the combined action of pancreatic, T1, and T2 RNases (Barrell, 1971) in 50 mM ammonium acetate, pH 4.5. The digest was analyzed by cellulose thin-layer chromatography in solvents that distinguish Up from Dp. These were as follows: solvent system B, 2-propanol–concentrated HCl–H_2O (68:17:15) (Nishimura, 1972); solvent system C, 0.1 M sodium phosphate, pH 6.8–$(NH_4)_2SO_4$–1-propanol (100:60:2) (Silberklang et al., 1977). Nucleotide 3′-monophosphates (Sigma) and pCp (P-L Biochemicals) were chromatographed in parallel and visualized with ultraviolet light.

RNase A Digestion. The 3′-^{32}P end-labeled fragment was digested with pancreatic RNase in 10 mM Tris-HCl, pH 7.4–1 mM EDTA. Digestion products were analyzed by cellulose thin-layer chromatography in solvent systems A and C to verify the nucleotide sequence at the Pb(II) cleavage site.

X-ray Crystallography. The crystals were stored in a buffer consisting of 15 mM $MgCl_2$, 1.5 mM spermine tetrahydrochloride, and 10 mM Tris-HCl (pH 7.4), and 20% hexane-1,6-diol was added prior to the addition of $Pb(OAc)_2$ to overcome the problem of the crystals cracking. To this was added slowly, over several hours, a solution of 10 mM $Pb(OAc)_2$ until the final Pb(II) concentration was 1 mM to give a ratio of five Pb(II) ions per tRNA^{Phe} molecule.

Data to 3-Å resolution were collected on a Hilger-Watts four-circle diffractometer using Ni-filtered Cu-Kα radiation. Data collection was carried out at −5 °C with a cooling device consisting of a mechanically refrigerated dry airflow mounted on the χ circle of the diffractometer and coincident with the ϕ axis. Data, including Friedel pairs, were collected in spherical shells of reciprocal space by the ω step–scan technique with, typically, 26 steps at 0.03° intervals being used. For the low-resolution stronger data, counting was for 3 s per step (ca. 1 min/reflection), which was gradually increased to 7 s per step for the high-resolution weaker data (ca. 3 min/reflection). Radiation damage was monitored and corrected for linearly, by measuring the 060, 004, and 400 reflections every 100 data. A total of 10 704 reflections were collected, and symmetry equivalents, including Friedel pairs, were merged together to give 4821 independent reflections. The intensity data were corrected for Lorentz and polarization effects and for absorption by the method of North et al. (1968).

For the experiment at pH 7.4, two crystals were used. For each crystal the complete *h0l* zone from 3 to 30 Å was collected and used to scale the data together. The first crystal, which was soaked in Pb(II) solution for 2 days, was used to collect data from 3.0 to 3.2 Å. The second crystal, soaked for 7 days, was used for the remainder of the data collection. Two difference Fourier projections, using the *h0l* zones from both crystals and native phases refined to $R = 21\%$, were computed. Both projections had essentially the same features, indicating the reliability of the data. A three-dimensional difference Fourier map using coefficients $|F_{Pb}| - |F_{native}|$ and native phases was computed.

For the experiment at pH 5.0, the buffer containing the crystals at pH 7.4 was exchanged for a buffer at pH 5.0, which consisted of 15 mM $MgCl_2$, 1.5 mM spermine tetrahydrochloride, 10 mM KOAc (pH 5.0), and 20% hexane-1,6-diol. In a preliminary investigation crystals were soaked for several days in a $Pb(OAc)_2$ solution at a Pb(II):tRNA^{Phe} ratio of ca. 5:1. Collection of the centrosymmetric *h0l* zone of reflections on the diffractometer and calculation of a difference Fourier map using coefficients $|F_{Pb}| - |F_{native}|$ and native phases showed that three Pb(II) ions were bound to the tRNA at similar positions and at roughly comparable occupancies as observed at pH 7.4. Crystallographic verification that strand scission had not occurred to any significant extent could only be obtained from a complete three-dimensional data set, however. To ensure that crystals were soaked in the $Pb(OAc)_2$ solution for as short a time as possible, thus minimizing strand cleavage, but to ensure maximum possible occupancy of the three Pb(II) sites, a batch of crystals was soaked for 24 h as above and an *h0l* zone again collected. This required about 2 days on the diffractometer at −5 °C. A difference Fourier map showed the same Pb(II) occupancy as the crystals soaked for the longer time, indicating that 24 h was a sufficient time to obtain good occupancy of the Pb(II) binding sites, and preliminary biochemical experiments had shown that strand scission during this time at pH 5.0 would be less than 10%.

Four crystals were used for the data collection and each was soaked for only 24 h in the Pb(II) solution prior to the commencement of data collection. For scaling purposes a block of ca. 100 common *h0l* reflections was collected for each of the seven shells of data. No crystal decayed in the X-ray beam by more than 15% of its initial intensity, and no crystal was used for data collection beyond 6 days. A total of 10 778 reflections was collected and merged to give 4893 independent reflections.

Results

Crystallographic Results

The difference Fourier map between the Pb(II) derivative at pH 7.4 and native tRNA structure showed only four peaks of significance. Three of these peaks had positive electron density and were interpreted as Pb(II) ions bound to the tRNA^{Phe} molecule. The fourth peak was of negative electron density (Figure 2a), was situated at the position of phosphate-18, clearly incorporates the phosphorus atom and surrounding four oxygen atoms of the phosphate anion, and is interpreted to mean that phosphate-18 has either moved or is absent from the Pb(II) derivative at pH 7.4, that is, that the sugar–phosphate backbone of the tRNA^{Phe} molecule has been cleaved at this point. Apart from these four peaks the difference Fourier map was featureless, indicating that there is good isomorphism between native and derivative structures and that the tRNA^{Phe} structure had not been changed markedly by the Pb(II) binding.

In order to try and extract the best possible coordinates, and hence geometry, for the Pb(II) ions and surrounding tRNA molecule, consistent with the resolution of the data and ad-

Table I: Crystallographic Coordinates (Å) and Occupancies (Electrons) of the Three Pb(II) Ions in the Two Crystal Structures of the Pb(II) tRNA^{Phe} Derivatives[a]

	x	y	z	occupancy
Pb(1)	52.85	10.80	32.70	24
	(52.62)	(10.91)	(32.62)	(50)
Pb(2)	46 46	8.57	16.40	34
	(46.45)	(8.43)	(16.26)	(40)
Pb(3)	44.45	−10.28	−1.21	61
	(44.50)	(−10.36)	(−1.20)	(63)

[a] Values for the structure at pH 5.0 appear in parentheses below those for the structure at pH 7.4.

ditional problems due to the partial occupancy of the Pb(II) ion sites, the derivative structure was subjected to several cycles of Jack–Levitt refinement (Jack & Levitt, 1978). The coordinates of the Pb(II) ions were not constrained in any way, but the tRNA molecule was constrained as described for the native refinement (Hingerty et al., 1978) except that phosphate-18 was removed from the coordinate list and a gap introduced into the sugar–phosphate backbone at this point. The initial coordinates were those of the native structure refined to $R = 21\%$. The R factor of the Pb(II) derivative data at pH 7.4 at the commencement of refinement was 30.3% and at convergence was 22.7%.

Approximately 10 cycles of positional refinement led to convergence. As judged by changes in the Pb(II)–ligand distances, however, this refinement had little effect on the overall structure. Four cycles of refinement of individual isotropic temperature factors again led to little change in the structure. After each cycle the temperature factors were averaged over each base and over each sugar–phosphate moiety. The coordinates of the Pb(II) ions so obtained appear in Table I. The three Pb(II) binding sites have been labeled Pb(1), Pb(2), and Pb(3).

A difference Fourier map for the experiment at pH 5.0 was computed as before and showed only three positive peaks of any significance. These corresponded to Pb(II) bound to the tRNA molecule in very similar positions to that observed in the structure at pH 7.4. The negative peak observed in the structure at pH 7.4 was absent in the structure at pH 5.0, indicating that strand scission had not taken place to any observable extent at this latter pH (Figure 2b). In the Jack–Levitt refinement, therefore, the sugar–phosphate backbone at phosphate-18 was left intact. The positions of the Pb(II) ions obtained from the refinement appear in Table I. The R factor at the commencement of refinement was 31.4% and that at convergence was 23.7%.

The metal ion occupancies of each Pb(II) binding site were also refined, for each pH. The coordination sphere of each Pb(II) ion presumably contains a number of water molecules to complete its coordination shell since the number of coordination sites that are occupied by binding to the tRNA molecule is only one or two for each Pb(II) ion. The number of such water molecules is very difficult to assess, however, since the coordination number and coordination geometry of Pb(II) is quite variable (Harrison, 1976). In the present case we have not attempted to place water molecules around each Pb(II) ion, have treated each Pb(II) ion at full occupancy as having 80 electrons, and have refined the occupancy from this as a starting point. The occupancies thus obtained appear in Table I. The structures at pH 7.4 and pH 5.0 were both scaled to the native data so that the occupancies for these Pb(II) derivatives are directly comparable.

The three Pb(II) ions replace various other species upon binding to the tRNA^{Phe} molecule. At site Pb(1) a Mg(II) ion, designated as Mg(3) by Jack et al. (1977), is displaced. The Pb(1)···Mg(3) distance is only 2.1 Å, and it is unlikely that both metal ions bind simultaneously to the same tRNA molecule. We presume that when Pb(II) binds, the Mg(II) ion is displaced, since any density placed at the Mg(3) site vanished during refinement. At site Pb(2) a spermine molecule is replaced since the closest Pb(2)···spermine distance would be 1.7 Å, and again, it is unlikely that both species would be bound simultaneously. The Pb(II) ion at site Pb(2) binds at the same position as Sm(4) in the paper of Jack et al. (1977). At site Pb(3) a water molecule is displaced (Hingerty et al., 1980). In the orthorhombic tRNA^{Phe} crystal structure this peak has been assigned as a Mg(II) ion (Holbrook et al., 1977).

The occupancies at site Pb(2) are similar at either pH, which is also the case at site Pb(3). At site Pb(1), however, the occupancy at pH 7.4 (after the cleavage reaction) is significantly lower than that at pH 5.0 (before the cleavage reaction). We have taken this to mean that after chain cleavage the folded structure of the RNA in this region is weakened, leading to reduced binding of the Pb(II) ion. The corollary of this is that the reaction is catalytic, since the Pb(II) ion released can migrate to another molecule or to another site in the same molecule. This point is taken up in more detail below.

The negative peak at phosphate-18 in Figure 2a represents strand cleavage. If so, why do we not see a new positive peak nearby to represent the position to which this phosphate group has moved? One explanation could be that the phosphate has been completely excised from the tRNA, which would require two cleavages of the sugar–phosphate backbone. This seems unlikely and does not fit with our biochemical end-group analysis. Another possibility could be that the negative peak represents removal of not only phosphate-18 but also ribose-17 and the base D-17. This would arise from a cleavage between D-17–G-18 followed by another between D-16–D-17, which we do indeed find at late stages in the hydrolysis (see below). The difference map at pH 7.4, however, only shows weak negative electron density encompassing ribose-17 and D-17, and a difference map with ribose-17 and D-17 left out of the phase calculations had positive peaks in the vicinity of these two groups, suggesting that they were present.

We think that the explanation for the absence of a positive peak accompanying the negative one lies in the fact that the Pb(II)-soaked crystal as we observe it at pH 7.4 has only about 50% of its D-17–G-18 bonds cleaved (see below) and does not represent a simple final state of the cleaved molecule. As discussed below in the section on the biochemistry and as depicted in Figure 10, we expect the cleavage to take place in a number of stages, through a cyclic phosphate intermediate. The crystal structure would then represent a mixture or superposition of these intermediates, rather than show the final position of the phosphate group (a movement of about 3 Å on the model shown in Figure 10), and hence, the shifted phosphate peak would be smeared out and unobservable above background in the difference Fourier map. The negative peak would of course still show the full effect.

It should perhaps be emphasized that it would not have been possible to reach a simple final stage in the crystallographic experiments. As explained below, the Pb(II)-mediated cleavage proceeds beyond the first cleavage at bond D-17–G-18, to cut the bond D-16–D-17. We therefore used short times of cleavage for the crystal data collection, so that we could be sure of catching the first bond cleaved.

The Pb(II) Binding Sites. Three Pb(II) ions bind to the tRNA^{Phe} molecule, and the binding sites are the same at pH

Table II: Distances (<7 Å) from the Three Pb(II) Ions to All N, O, and P Atoms of the $tRNA^{Phe}$ Molecule[a]

Pb(1)		Pb(2)		Pb(3)	
atom	distance (Å)	atom	distance (Å)	atom	distance (Å)
O2′ (G-15)	5.3	N1 (A-9)	4.9	N6 (A-31)	5.2
N2 (G-15)	6.2	N6 (A-9)	6.2	N1 (A-31)	6.0
N3 (G-15)	6.2	N3 (A-9)	6.4	N7 (A-31)	6.9
OL (D-16)	4.8	O2′ (A-21)	6.7	O2 (Cm-32)	2.9
O1′ (D-16)	5.0	OL (G-22)	5.4	N3 (Cm-32)	4.0
P (D-16)	6.0	O5′ (G-22)	5.7	N1 (Cm-32)	5.2
O3′ (D-16)	6.1	P (G-22)	6.2	N4 (Cm-32)	5.9
O2 (D-16)	6.2	OR (G-22)	6.6	O2′ (Cm-32)	6.2
N1 (D-16)	6.3	OL (A-23)	4.8	O2 (U-33)	3.6
O5′ (D-16)	6.3	P (A-23)	6.1	N1 (U-33)	5.0
N3 (D-16)	6.4	O3′ (A-23)	6.2	N3 (U-33)	5.0
O2′ (D-17)	6.0	OR (A-23)	7.0	O1′ (U-33)	5.5
OR (D-17)	6.8	O5′ (G-43)	6.8	O2′ (U-33)	6.2
O5′ (G-18)	5.9	OL (G-43)	6.8	O4 (U-33)	6.8
O1′ (G-18)	6.3	OL (A-44)	4.1	N7 (A-35)	6.4
OR (G-19)	3.4	N7 (A-44)	4.7	N6 (A-35)	6.5
P (G-19)	4.9	P (A-44)	5.5	N7 (A-36)	3.1
O3′ (G-19)	5.6	N6 (A-44)	5.9	N6 (A-36)	3.4
O5′ (G-19)	5.7	O5′ (A-44)	5.9	N9 (A-36)	5.0
OL (G-19)	5.8	OR (A-44)	6.0	N1 (A-36)	5.1
O6 (G-20)	4.4	N9 (A-44)	6.4	O5′ (A-36)	5.4
N7 (G-20)	5.0	O3′ (A-44)	6.6	OL (A-36)	5.4
N1 (G-20)	6.7	O6 (G-45)	2.5	N3 (A-36)	5.8
OL (G-20)	6.8	N7 (G-45)	3.6	P (A-36)	6.2
O4 (U-59)	2.2	N1 (G-45)	4.6	O1′ (A-36)	6.4
N3 (U-59)	3.6	N9 (G-45)	5.9	N7 (Y-37)	2.4
O2 (U-59)	5.5	N3 (G-45)	6.1	O6 (Y-37)	3.2
N1 (U-59)	5.6	N2 (G-45)	6.9	N9 (Y-37)	4.7
O1′ (U-59)	7.7	O6 (m^7G-46)	6.7	N1 (Y-37)	5.1
N3 (C-60)	2.8			N3 (Y-37)	5.9
N4 (C-60)	3.5			OL (Y-37)	6.1
O2 (C-60)	3.6			O1′ (Y-37)	6.3
N1 (C-60)	4.9			O5′ (Y-37)	6.7
O1′ (C-60)	6.7			P (Y-37)	7.0
				N6 (A-38)	4.3
				N7 (A-38)	4.4
				N1 (A-38)	5.9
				N9 (A-38)	6.4
				N3 (A-38)	6.9
				OL (A-38)	6.9
				O2 (Ψ-39)	5.7
				N1 (Ψ-39)	6.9
				N3 (Ψ-39)	6.9

[a] Atom labels include the residue type and sequence number in parentheses.

5.0 and pH 7.4. The refined coordinates of these Pb(II) ions appear in Table I, and an overall diagram showing the Pb(II) binding sites appears as Figure 3. They occur in complexly folded regions of the molecule. A similar diagram depicting the binding sites of various other metal ions is shown in Figure 11 of Jack et al. (1977). Site Pb(1) is close to the cleavage site between residues D-17 and G-18 in the crystal structure at pH 7.4 (Figure 2a). No strand cleavage is observed near sites Pb(2) and Pb(3).

The metal ion was added to the $tRNA^{Phe}$ crystals as Pb(II), and we have assumed that this oxidation state is maintained since it will be preferred over Pb(IV) in aqueous media. The structural chemistry of Pb(II), published prior to about 1976, has been reviewed (Harrison, 1976). The number of small molecule structures that are particularly relevant to Pb(II) binding to $tRNA^{Phe}$ is quite small, and indeed, the total number of structure determinations on Pb(II) compounds is not large. Also, no Pb(II) complexes with nucleic acid bases have thus far been structurally characterized although such complexes with other metals abound (Hodgson, 1977; Swaminathan & Sundaralingam, 1979; Marzilli et al., 1980).

The structural chemistry of Pb(II) is not straightforward and is characterized by a range of coordination numbers and a wide variety of coordination geometries. Coordination numbers up to 12 are known for Pb(II), albeit in compounds such as $Pb(NO_3)_2$ and $PbSO_4$ (Harrison, 1976). Another factor that complicates the coordination geometries (i.e., stereochemistries) of Pb(II) compounds is the lone pair of electrons on the metal. It is not possible to predict whether or not this lone pair is stereochemically active. An excellent example of this occurs in the recently determined structure of a Pb(II)–EDTA complex (Harrison et al., 1982; Harrison & Steel, 1982). The structure contains two crystallographically independent Pb(II) ions, one of which is seven-coordinate while the other is eight-coordinate. The lone pair of electrons is stereochemically active on the seven-coordinate Pb(II) ion but appears to be stereochemically inactive on the eight-coordinate Pb(II) ion. It is for these reasons just mentioned that we have decided that an attempt to place water ligands on each Pb(II) ion would be a fruitless exercise in the present case.

Pb(1) Binding Site. At this site a Pb(II) ion is bound in the TΨC loop of the $tRNA^{Phe}$ molecule as depicted in Figures 3 and 4a,b. There is a direct bond to O4 of U-59 at 2.2 Å and to N3 of C-60 at 2.8 Å. Other contacts less than 4 Å are to OR of phosphate-19 at 3.4 Å, N4 and O2 of C-60 at 3.5 and 3.6 Å, respectively, and N3 of U-59 at 3.6 Å (Table II).

The Pb(1)–N3(C-60) distance of 2.8 Å is quite comparable to similar Pb(II)–N(aromatic) distances observed in a variety

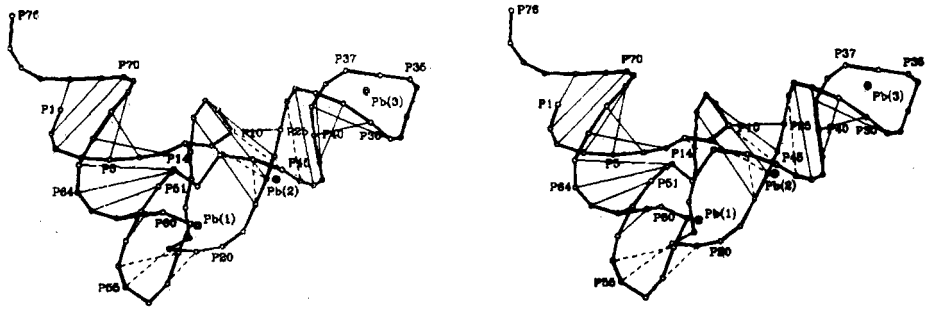

FIGURE 3: Stereoview of yeast tRNA^{Phe} showing the locations of the three Pb(II) binding sites where Pb(1) is bound to U-59 and C-60, Pb(2) to G-45, and Pb(3) to Y-37. The backbone of the molecule is represented by a heavy line joining successive phosphorus atoms of each phosphate group. Certain of the phosphorus atoms are labeled along with their sequence number. Single unbroken lines join phosphorus atoms whose bases are paired in Watson–Crick double-helical regions. Single broken lines join phosphorus atoms of other pairs of hydrogen-bonded bases.

of small-molecule complexes that have been structurally characterized (Cingi et al., 1972, 1975; Kon & Bourshteyn, 1976; Lerner & Lippard, 1977; Drew et al., 1978; Beveridge & Bushnell, 1979; Drew & Nelson, 1979; Pierce-Butler, 1982). The Pb(1)–O4(U-59) distance of 2.2 Å would appear to represent a strong bonding interaction being at the short end of the range for similar Pb(II)–O(carbonyl) distances in small molecule complexes (Vijayan & Viswamitra, 1966; Yu & Fritchie, 1975; White & Willis, 1977).

The closest contact between Pb(II) and a phosphate oxygen atom occurs at site Pb(1) where the Pb(1)···OR(G-19) distance is 3.4 Å. For site Pb(2) the closest such contact is 4.1 Å to OL(A-44), and for site Pb(3) the closest contact is 5.4 Å to OL(A-36). These distances are all rather long to be considered strong bonding interactions when comparison is made with Pb(II)–O(phosphate) distances in small-molecule compounds (Harrison, 1976). A similar situation was noted in the structure of staphylococcal nuclease where a Ca···O(phosphate) distance of ca. 3 Å was considered to be too long to allow any strong interaction or direct coordination (Arnone et al., 1971).

The binding of Pb(II) to O4(U-59) is very similar to the binding of Hg(II) to O4(U-47) (Jack et al., 1977), where the Hg(II) was added as the compound (hydroxymercuri)hydroquinone *O,O*-diacetate (HMHD), and the binding of mercury to uracil in the small-molecule compound formed with $HgCl_2$ (Carrabine & Sundaralingam, 1971). In the HMHD and $HgCl_2$ cases, the Hg(II) ion is 1.5 Å out of the plane of the uracil base, and in the present case, Pb(1) is 1.3 Å from the plane of U-59. Atom Pb(1) is also bonded to N3(C-60) and lies 1.0 Å from the plane of C-60. The Pb(II) ion is intermediate in character between a hard and soft metal (Ahrland et al., 1958; Pearson, 1963) and in this case seems to be sharing its binding between the hard carbonyl oxygen atom of U-59 and the softer aromatic nitrogen of C-60.

The binding of the Pb(II) ion at site Pb(1) replaces a Mg(II) ion bound in this vicinity in the native structure. The Mg(II) ion replaced was designated Mg(3) in the paper of Jack et al. (1977) and is bound directly to phosphate oxygen OR(G-19) at 1.6 Å. The Pb(1)···Mg(3) distance is only 2.1 Å, and obviously, both metal ions do not exist together in the same molecule. In a separate experiment Mn(II) has also been found to bind in this region, forming a direct bond to N7 of the base G-20 at 2.3 Å (Jack et al., 1977). The Mn(II) ion presumably replaces Mg(3) when it binds to the tRNA^{Phe} molecule in a manner similar to Pb(II).

Pb(2) Binding Site. At this site a Pb(II) ion is bound in the extra loop region of the tRNA^{Phe} molecule as shown in Figures 3 and 4c. There is a direct bond to O6(G-45) at a distance of 2.5 Å with a further contact to N7(G-45) at 3.6 Å. All other contacts are greater than 4.0 Å (Table II). The Pb(2)–O6(G-45) distance of 2.5 Å represents a strong bonding interaction being at the shorter end of the range for Pb(II)–O(carbonyl) distances.

At site Pb(2) the Pb(II) ion displaces a spermine molecule that is bound in this vicinity in the native structure. In other experiments the complex cation $[Co(NH_3)_6]^{3+}$ replaces spermine and binds in this region via an extensive hydrogen-bonding network. The lanthanides Sm(III) and Lu(III) also bind in this region, and the site is labeled Sm(4) in the paper of Jack et al. (1977). The lanthanides bind at five sites in the tRNA^{Phe} molecule, and four of these involve direct binding to phosphate oxygen atoms. At the Sm(4) site, however, the lanthanides bind in exactly the same manner as does the Pb(II) ion, that is, via a direct bond to O6(G-45) with a long contact to N7 of the same base. The distances involved for the lanthanides are lanthanide–O6(G-45) = 2.4 Å and lanthanide···N7(G-45) = 3.3 Å.

Pb(3) Binding Site. The Pb(II) ion at this site is bound in the anticodon loop of the tRNA^{Phe} molecule as depicted in Figures 3 and 4d. There is a direct bond to N7(Y-37) of 2.4 Å with longer contacts, less than 4.0 Å, to O2 of Cm-32 at 2.9 Å, N7(A-36) at 3.1 Å, O6(Y-37) at 3.2 Å, N6(A-36) at 3.4 Å, and O2(U-33) at 3.6 Å (Table II). The Pb(3)–N7(Y-37) distance of 2.4 Å represents a strong bonding interaction and is quite comparable to similar distances noted above in a number of small-molecule compounds.

It is interesting that at site Pb(3) the Pb(II) ion binds to N7 of the Y base [Pb(3)–N7(Y-37) = 2.4 Å] rather than to O6 [Pb(3)···O6(Y-37) = 3.2 Å] whereas at site Pb(2), where a very similar binding site is presented, the Pb(II) ion binds to O6 of guanine [Pb(2)–O6(G-45) = 2.5 Å] rather than to N7 [Pb(2)···N7(G-45) = 3.6 Å]. As mentioned above site Pb(1) involves binding to a carbonyl oxygen and an aromatic nitrogen atom. The only small-molecule structure that presents a similar mixed binding site is in the Pb(II) complex with 10-methylisoalloxazine (Yu & Fritchie, 1975) where Pb(II) binds preferentially to the carbonyl oxygen rather than to the aromatic nitrogen atom. The Pb(II) ion is borderline between being a hard or soft metal (Ahrland et al., 1958; Pearson, 1963), and it would appear from the tRNA^{Phe} derivative structures that there is little observable preference for it to bind to either the hard carbonyl oxygen or the softer aromatic nitrogen atom.

The Pb(II) ion at site Pb(3) displaces a water molecule located in this region (Hingerty et al., 1980). In the native orthorhombic crystals a $[Mg(H_2O)_6]^{2+}$ ion has been assigned to this region and is presumed to hydrogen bond to Y-37 (Holbrook et al., 1977).

Consideration of Pb(II)–Water Interactions. Distances of 5–6 Å (Table II) between Pb(II) and suitable hydrogen-bond acceptor atoms of the tRNA^{Phe} molecule should represent instances where water is bound directly to Pb(II) and also

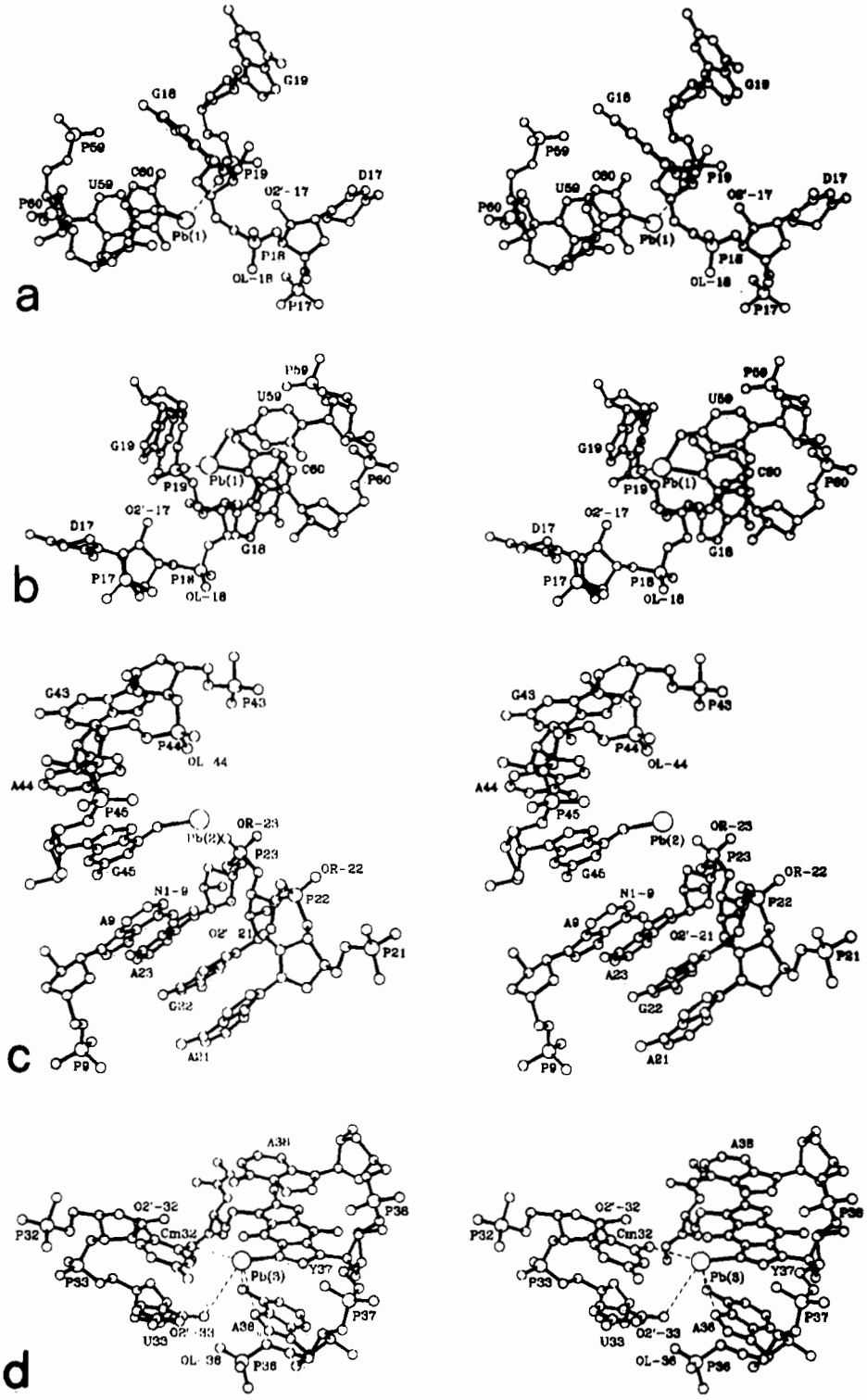

FIGURE 4: Stereoviews of the three Pb(II) ion binding sites in crystalline $tRNA^{Phe}$. Each base and phosphorus atom is labeled, including its sequence number, and certain of the other atoms are also labeled. (a and b) Site Pb(1), the cleavage site, where the Pb(II) ion is bound to O4(U-59) and N3(C-60) with a long contact (dashed line) to OR(P-19). In (a) the view of the sugar–phosphate backbone is similar to that depicted in Figure 10. (c) Site Pb(2) where the Pb(II) ion is bound to O6(G-45). (d) Site Pb(3) where the Pb(II) ion is bound to N7(Y-37) with long contacts (dashed lines) to O2(Cm-32), O2(U-33), N6(A-36), and N7(A-36).

hydrogen bonds to the tRNA. Precedents for these distances exist (Cingi et al., 1972; Yu & Fritchie, 1975; White & Willis, 1977; Beveridge & Bushnell, 1979; Drew et al., 1979; Houttemane et al., 1981; Harrison et al., 1982; Harrison & Steel, 1982).

Biochemical Characterization of the Cleavage Site

The action of Pb(II) on several tRNA species from yeast has been studied in detail by Werner et al. (1976). In these experiments cleavage sites were identified by RNase T1 fingerprint analysis of the fragments obtained in the presence of 0.5 or 1 M NaCl. In $tRNA^{Phe}$ cleavage was found to occur primarily between residues D-17 and G-18 and to a lesser extent between D-16 and D-17. Although our X-ray analysis suggests a single cleavage site between D-17 and G-18, it is not possible at 3-Å resolution to identify the chemical nature of the end groups present at this site. We undertook, therefore, a biochemical characterization of the fragments produced by

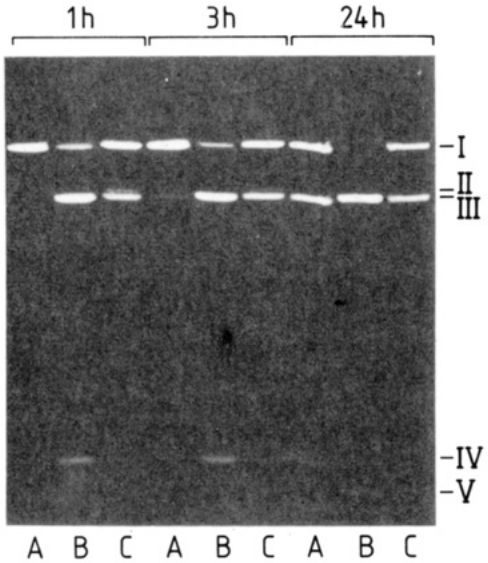

FIGURE 5: Effect of pH on Pb(II)-induced cleavage of brewers' yeast tRNA^{Phe} in solution. Analysis by 18% polyacrylamide–7 M urea gel electrophoresis reveals the fragments obtained after 1, 3, and 24 h at pH 5.0 (lane A), at pH 7.4 (lane B), and at pH 9.0 (lane C). tRNA^{Phe} (20 μM) was treated with 100 μM $Pb(OAc)_2$ at room temperature. The major cleavage products were identified as the one-fourth fragment G-1–D-17 (band IV) and the three-fourth fragment G-18–A-76 (band III). Band I is intact tRNA^{Phe}. Minor products are probably: G-1–D-16 (band V) and D-17–A-76 (band II). [Gel bands I and III can be resolved into doublets by continuing electrophoresis for a longer time, because native tRNA^{Phe} contains a minor component that has lost its terminal 3′-nucleotide—see text (RajBhandary et al., 1968).] At still later times, band I disappeared, and band IV was gradually converted into band V. The gel was stained with ethidium bromide to locate the fragments.

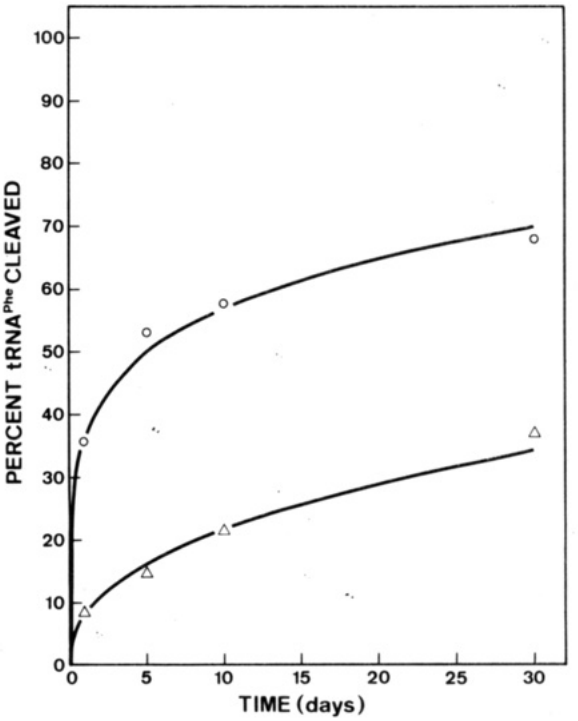

FIGURE 6: Time course of the Pb(II) cleavage reaction in monoclinic crystals of tRNA^{Phe} at 4 °C at a ratio of Pb(II):tRNA^{Phe} of 5:1. Crystals were soaked in 1 mM $Pb(OAc)_2$ and removed at intervals for analysis by polyacrylamide gel electrophoresis as described under Materials and Methods. The percentage of tRNA^{Phe} molecules cleaved at pH 5.0 (△) and at pH 7.4 (○) was estimated visually from gel bands stained with ethidium bromide.

the action of Pb(II) in crystals of tRNA^{Phe}.

Gel Analysis of Pb(II) Reaction Conditions. In agreement with the X-ray analysis, the major products of Pb(II) cleavage in crystals of tRNA^{Phe} at pH 7.4 were found by polyacrylamide gel electrophoresis to be a one-fourth and a three-fourth fragment of the molecule (Figure 5). This fragmentation was also observed in solution at 4, 22, and 37 °C and remained unaltered over a range of $Pb(OAc)_2$ concentration from 5 μM to 10 mM. The influence of pH is also shown in Figure 5 where the cleavage reaction occurs considerably faster at pH 7.4 than at pH 5.0 or pH 9.0.

Similar results to those in solution were obtained in crystals of tRNA^{Phe} at 4 °C. The time course of the reaction is shown in Figure 6 where the ratio of Pb(II) to tRNA^{Phe} was 5:1. After a soaking time of 70 days, the reaction proceeds to about 48% cleavage of tRNA^{Phe} at pH 5.0 and 82% cleavage at pH 7.4 (data not shown). Thus, crystals used for the X-ray data collection at pH 5.0 contained tRNA^{Phe} with less than 10% cleavage and those at pH 7.4 about 50% cleavage.

It should be noted that the bands corresponding to the full-length and three-fourth molecules in the electrophoresis patterns in Figure 5 are really doublets, which can be resolved by running the electrophoresis for longer times. This is because a typical native tRNA^{Phe} preparation consists of two components, a full-length molecule of 76 nucleotides and a fraction, typically about 10%, which has lost its terminal pA group, leaving a 3′-OH on residue 75 (RajBhandary et al., 1968). This produces leading minor peaks in bands I and III (Figure 5) in the longer electrophoresis runs.

The Pb(II) cleavage experiments in 10 mM Tris-HCl at pH 9.0 were carried out for completeness, although we have no companion crystallographic data. The reaction is slower than that at pH 7.4, which we attribute to the much greater insolubility of the Pb(II) ions, due to the formation of polyhydroxo species (Kepert, 1970; Baes & Mesmer, 1976; Sylva & Brown, 1980), which renders them less effective. A somewhat different pattern of cleavage is observed. A trailing minor band now accompanies the three-fourth molecule band, and the one-fourth band is split into a clear doublet (bands IV and V in Figure 5). This is because the minor cleavage between D-16 and D-17, which is only revealed with time at pH 7.4, becomes at pH 9.0 comparable with the cleavage between D-17 and D-18. Hence, two fragments of length 16 and 17 nucleotides, respectively, are seen (bands IV and V). Thus the relative susceptibility of the two cleavages changes in a way similar to that found by Werner et al. (1976), when the salt conditions are varied.

5′ End Group. [5′-^{32}P]pG was released by nuclease P1 digestion from the 5′-^{32}P end-labeled three-fourth fragment (band III in Figure 5). Prior treatment of the three-fourth fragment with calf intestinal alkaline phosphatase did not result in any significant increase in radioactivity incorporated by T4 polynucleotide kinase. This indicates that a guanine residue is present at the 5′-terminus with a free 5′-OH group (Figure 7a). An unambiguous identification of the nucleotide at the 5′-terminus was obtained by two-dimensional homochromatography (see Figure 7b). The 5′-nucleotide sequence adjacent to the cleavage site was found to be G-G-G-A-G-A-G-C-, showing that the cleavage took place before residue G-18 (cf. sequence in Figure 1) in complete agreement with the X-ray crystallographic analysis.

A small amount of [5′-^{32}P]pA was detected in phosphatase-treated samples. However, this was shown to originate not from a minor Pb(II) cleavage site in tRNA^{Phe} between residues G-22 and A-23 as previously supposed by us (Brown et al., 1983) but results from RNase contamination in the commercial calf intestinal alkaline phosphatase. The minor

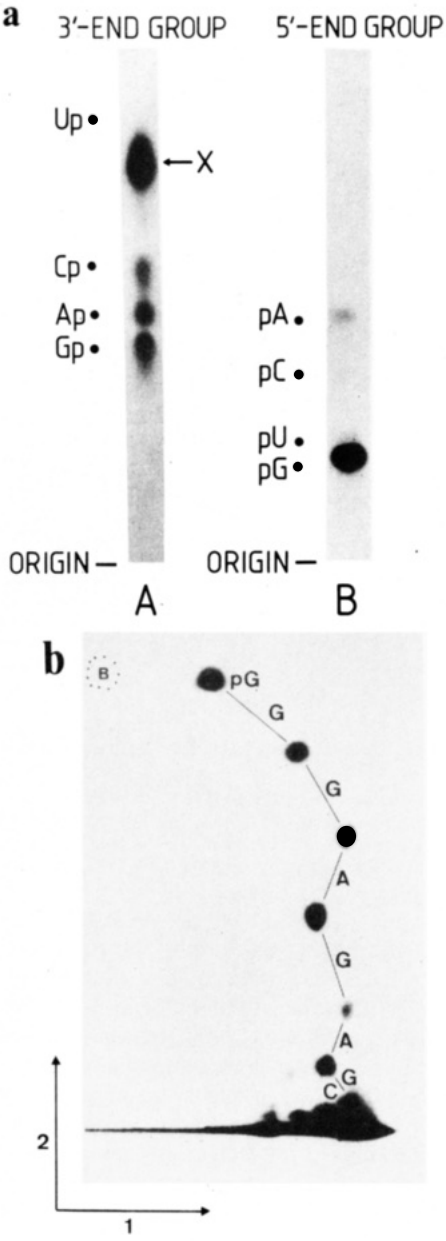

FIGURE 7: (a) End-group analysis at the site of Pb(II)-catalyzed cleavage in crystals of yeast $tRNA^{Phe}$. (A) Autoradiogram of the labeled terminal nucleotide from the 3′-^{32}P-labeled one-fourth fragment after thin-layer chromatography in solvent system B as detailed under Materials and Methods. After chromatography the marker nucleotides were visualized under UV light. The major product (X) migrated slower than uridine 3′-monophosphate and is identified as dihydrouridine 3′-monophosphate (Nishimura, 1972). (B) Autoradiogram of the labeled terminal nucleotide from the 5′-^{32}P-labeled three-fourth fragment after thin-layer chromatography in solvent system A. (b) The 5′-terminal nucleotide sequence adjacent to the Pb(II) cleavage site in $tRNA^{Phe}$ determined by the so-called "wandering spot" method (Walker & RajBhandary, 1975). The autoradiogram shows the two-dimensional separation of nuclease P1 partial digestion products obtained from the 5′-^{32}P-labeled three-fourth fragment of $tRNA^{Phe}$. The first dimension was ionophoresis on cellulose acetate at pH 3.5 for 1 h at 4 kV. The second dimension was homochromatography on a DEAE-cellulose thin layer at 65 °C. The circled B indicates the position of the blue dye marker xylene cyanol.

component of band III in Figure 5 was also found to have a guanine residue at its 5′-terminus.

3′ End Group. The products of alkaline hydrolysis of RNA are a cyclic 2′,3′-phosphate and a free 5′-OH group. Farkas (1968) identified adenosine cyclic 2′,3′-phosphate as the product of the Pb(II) degradation of poly(A). Hence, a strategy was devised to reveal the presence of a cyclic 2′,3′-phosphate at the 3′-terminus of the one-fourth fragment of $tRNA^{Phe}$. Advantage was taken of the property of the enzyme T4 RNA ligase to add [5′-^{32}P]pCp to the 3′-terminal nucleotide –N, when a free 3′-OH group is present. Subsequent digestion with a combination of T1, T2, and pancreatic RNase results in the release of the 3′-terminal nucleotide [3′-^{32}P]Np. We obtained a single radioactive product on digestion of the one-fourth fragment, which had been treated with both 0.1 M HCl and calf intestinal alkaline phosphatase before incubation with T4 RNA ligase and [5′-^{32}P]pCp. Analysis by thin-layer chromatography in solvent systems B (Nishimura, 1972) and C (Silberklang et al., 1977) identified dihydrouridine as the 3′-terminal nucleotide (Figure 7a). No radioactivity was incorporated into the untreated one-fourth fragment. However, a small amount of [3′-^{32}P]Dp was obtained from the control sample that had undergone the calf intestinal alkaline phosphatase treatment. We infer from these results that the 3′-end-labeling reaction is blocked by the presence of a cyclic 2′,3′-phosphate group.

Sequence Adjacent to 3′-Terminus. There are two dihydrouridine residues in the sequence of yeast $tRNA^{Phe}$ at positions 16 and 17. It can be seen that RNase A digestion of the ^{32}P-labeled one-fourth fragment G-1···C-13–A-14–G-15–D-16–D-17*pCp yields D*p whereas digestion of G-1···C-13–A-14–G-15–D-16*pCp gives A-G-D*p. The radioactive products of RNase A digestion were idenitified by thin-layer chromatography as a mixture of D*p and A-G-D*p approximately in the ratio of 1:10. Thus, the one-fourth fragment appears to be mainly the sequence G-1–D-16 although the X-ray analysis indicates a single cleavage site between residues D-17 and G-18 and the 5′ end group is unambiguously G-18. This discrepancy may be in part due to the fraying action of 0.1 M HCl on the one-fourth fragment. Some random or nonspecific breakdown was observed, and it is not known to what extent the linkage between residues D-16 and D-17 is susceptible to dilute acid. However, the most likely explanation of the discrepancy is that the material used for the biochemical analysis was obtained from crystals exposed for 3 weeks to 1 mM $Pb(OAc)_2$ at pH 7.4, whereas the crystals used for X-ray data collection were soaked for only 2 and 7 days, respectively. Prolonged treatment with Pb(II) was found to cause the conversion of the one-fourth fragment to a slightly smaller fragment, such as can be seen in Figure 5 (band V). It is likely that the sample used for analysis, which was recovered from a preparative 15% polyacrylamide gel, was in fact an unresolved mixture of these.

DISCUSSION

Mechanism of the Cleavage Reaction. Our crystallographic investigations of Pb(II) binding to monoclinic crystals of $tRNA^{Phe}$ show that the metal ion binds to the same three sites at pH 5.0 and pH 7.4 and that site Pb(1) is very close to that region of the tRNA found, in our biochemical work and that of others (Werner et al., 1976), to be cleaved by Pb(II) (Table I, Figures 2 and 3). In the absence of Pb(II), the tRNA is not cleaved, and therefore, the proximity of the Pb(1) site to the site of sugar–phosphate backbone cleavage between residues D-17 and G-18 strongly implicates this Pb(II) ion in the cleavage reaction. Of major importance in this context is the observation that phosphate-18 is enveloped by significant negative electron density in the difference Fourier map at pH 7.4, which signifies that at this pH we are witnessing the tRNA after sugar–phosphate strand cleavage has occurred (Figure 2a). These results provide a unique opportunity to evaluate possible mechanisms for the Pb(II)-catalyzed hydrolysis of the

tRNA^{Phe} at the D-17–G-18 cleavage site. To date, very little detailed information on the mechanisms of metal ion depolymerization of RNA is available even though, as listed in the introduction, quite an amount of work has been performed in this general area.

There are two general mechanisms by which a metal ion in a macromolecule can effect catalysis of a particular reaction (Fersht, 1977; Buckingham, 1977). These are (1) the electrophilic activation mechanism and (2) the metal ion acting as a source of OH^- ions at or near neutral pH. In the present work, the electrophilic activation mechanism would involve direct binding of Pb(II) to a phosphate oxygen atom (either OL or OR). The P–O bond is thereby polarized and a partial positive charge induced on the phosphorus atom. This will facilitate nucleophilic attack by a water molecule or a hydroxyl ion on P forming a cyclic 2′,3′-phosphate and a 5′-OH on the leaving group. This mechanism has been proposed before for the depolymerization of RNA by Zn(II) (Butzow & Eichhorn, 1971).

Aquo Pb(II) ions as a source of metal-bound hydroxyl groups [i.e., $(Pb–OH)^+$ moieties] can be thought of as leading to two possible reactions in the present work. First, direct attack of the Pb(II)-bound hydroxyl group on the phosphorus atom of the phosphate. This mechanism has been suggested for carbonic anhydrase where a Zn(II)-bound hydroxyl group attacks the carbon atom of CO_2 to produce HCO_3^- (Buckingham, 1977). A hydroxyl group bound to Ca(II) was proposed to attack directly the phosphate P atom of the substrate in staphylococcal nuclease (Arnone et al., 1971; Cotton et al., 1971) although more recent work has shown that this is probably not the case (Cotton et al., 1979). Second, the $(Pb–OH)^+$ moiety may act as a general base and abstract H^+ from the 2′-OH of the tRNA. The 2′-O^- thus formed is better able to perform a nucleophilic attack on the P atom of the neighboring phosphate group forming a ribose cyclic 2′,3′-phosphate and a 5′-OH on the leaving group. A mechanism similar to this is proposed for the first step in pancreatic RNase A, where the imidazole of histidine-12 acts as the general base to deprotonate the 2′-OH of the substrate (Roberts et al., 1969; Wlodawer et al., 1983).

There are, therefore, three possible mechanisms to consider for the Pb(II)-catalyzed hydrolysis in the present work: (1) the electrophilic activation mechanism; (2) direct attack on a P atom by a Pb(II)-bound hydroxyl group; (3) deprotonation, and thus activation, of a ribose 2′-OH group by a Pb(II)-bound hydroxyl group.

Consider first the electrophilic activation mechanism. Table II lists the distances between Pb(1) and all OL and OR phosphate oxygen atoms within a distance of 7 Å. The closest contact is Pb(1)···OR(G-19) = 3.4 Å and is rather long to be considered as a strong interaction (Figure 4a,b). A similar conclusion was reached by Arnone et al. (1971) for Ca···O-(phosphate) distances in staphylococcal nuclease. If this close contact were to lead to strand scission via the electrophilic activation mechanism, we would expect strand scission between residues G-18–G-19, which neither our biochemical nor crystallographic work agrees with. The next closest contact is Pb(1)···OL(D-16) = 4.8 Å, which should produce strand scission between G-15–D-16 if the electrophilic activation mechanism is operative. Our biochemical experiments do show a fraying of the 3′-end of the one-fourth fragment normally produced by the D-17–G-18 cleavage, but the next bond cleaved is D-16–D-17 (see above). All other Pb(1)···O-(phosphate) distances are greater than 5.8 Å. Thus it would seem that the two cleavages observed between D-17–G-18 and D-16–D-17 do not occur via the electrophilic activation mechanism.

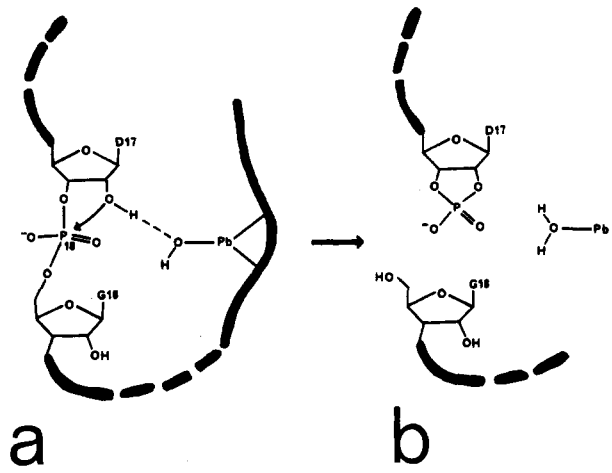

FIGURE 8: Diagrammatic representation of the proposed mechanism for the sugar–phosphate backbone cleavage between residues D-17 and G-18 in yeast tRNA^{Phe}. (a) Before strand cleavage. The [Pb-(II)–OH]$^+$ moiety is depicted as being bound to, and positioned by, the tRNA^{Phe} molecule. (b) After strand cleavage. The Pb(II)–OH_2 moiety is depicted as being free of the tRNA^{Phe} molecule.

The next mechanism to consider is the direct attack by a Pb(II)-bound hydroxyl group on a phosphate P atom. A Pb···P distance of ca. 5 Å would be required for such a mechanism since Pb–O distances can range up to ca. 3 Å (Harrison & Steel, 1982; Harrison et al., 1982) and an O···P distance of ca. 2 Å would be needed for direct reaction between these two atoms. The Pb(1)···P(G-19) = 4.9 Å contact is the shortest such distance and should lead to cleavage between G-18–G-19. This cleavage is not observed. The next shortest Pb(1)···P distance is 6.0 Å to P(D-16), which should lead to cleavage between G-15–D-16, but this is not observed. All other Pb-(1)···P distances are greater than 7.3 Å, and this mechanism can probably be ruled out for the D-17–G-18 cleavage.

The final possibility is abstraction of H^+ from a ribose 2′-OH group (Figure 8). This mechanism would require a Pb···O2′ distance of ca. 6 Å since Pb–O distances can range up to ca. 3 Å (Harrison & Steel, 1982; Harrison et al., 1982); the O-H distance is about 1 Å, and the H···O distance should be about 2 Å. The Pb(1)···O2′(D-17) distance is indeed 6.0 Å, and therefore, this would appear to be the most likely mechanism by which strand scission occurs at D-17–G-18 and is depicted schematically in Figure 8. All other Pb(1)···O2′ distances with the exception of Pb(1) to O2′ of G-15 are greater than 7.2 Å.

There is a proposed hydrogen bond between the proton of O2′(D-17) and OL(G-19), where the distance between these two latter atoms is 2.7 Å (Jack et al., 1976). If this hydrogen bond does exist, it would appear that it does not serve to prevent the cleavage between residues D-17–G-18.

RNA Cleavage Efficiency of Pb(II). It is known that Pb(II) cleaves RNA more efficiently than any other metal ion that has thus far been tested (Farkas, 1968, 1975). The principal reason for this unique behavior by Pb(II) may lie in the pK_1 value for this aquo metal ion where the pK_1 for a metal, M, is derived from eq 1. An examination of a comprehensive list

$$[(H_2O)_xM–OH_2]^{y+} = [(H_2O)_xM–OH]^{(y-1)+} + [H^+] \quad (1)$$

of such values for many metal ions (Burgess, 1978) shows that Pb(II) is rather different from most other metals as it has a pK_1 near 7 whereas other metals tend to have values either higher or lower than this. For example, the pK_1 for the lan-

thanides(III) is around 8.5, that for Zn(II) is around 9, and for Mg(II) the value lies near 12. This implies that Pb(II) should cleave RNA quite readily at or near neutral pH, provided a mechanism involving the $(Pb–OH)^+$ moiety is involved, while the other metals mentioned should require pH values significantly higher than this. Experiments on RNA and tRNA cleavage by Zn(II) and Mg(II), for example (Butzow & Eichhorn, 1971; Wintermeyer & Zachau, 1973), either have been conducted at pH values that are quite basic or involve elevated temperatures. We have found that treatment with 10 mM $Zn(OAc)_2$ at pH 7.4 and 37 °C does not cleave $tRNA^{Phe}$, whereas $Pb(OAc)_2$ under similar conditions gives complete cleavage at the major site.

For aquo metal ions with a pK_1 below 7, such as Al(III) and Fe(III), it might be expected that they would cleave RNA even more efficiently than Pb(II). It should be remembered, however, that metal ions such as these readily form polyhydroxo species and insoluble oxides at acidic pH values (Kepert, 1970), and this will prevent or severely curtail any tendency of the metal ion to cleave RNA.

Our consideration of pK_1 values, with regard to Pb(II) cleavage efficiency of RNA, is perhaps somewhat simplistic because the pK_a of a water molecule bound to a metal ion is often affected by the nature of the other ligands bound to that metal. In the present case, these other ligands represent the sites of attachment of Pb(II) to the $tRNA^{Phe}$ molecule. The effect of the other ligands is generally to lower the pK_a of the bound water molecule, and a good example of this has been reported in a Zn(II)–macrocycle complex (Woolley, 1975) where the pK_a of the water molecule bound to the Zn(II) ion is reduced from the normal value of ca. 9 to ca. 8. Another example has been reported by Groves & Dias (1979) where the pK_a of a Cu(II)-bound water molecule was found to be 7.6, which is much lower than the normal value of ca. 8.5. In the present case, however, a lowering of the pK_a would enhance the reaction rate of hydrolysis at pH 5.0 at site Pb(1), and this is not observed.

In our preliminary paper (Brown et al., 1983), we mentioned that, even though the pK_1 of Pb(II) is rather unique in that it falls around a value of 7, the reported pK_1 values of Cu(II) and Ni(II) also fall in this range. It would seem, however, that a value of 8.5 is more normal for Cu(II) (Groves & Dias, 1979) and that the wide 6.5–10.2 range given for Ni(II) would tend to indicate that some of the determinations of this value are inaccurate (Burgess, 1978).

Factors Required for Site-Specific $tRNA^{Phe}$ Cleavage. There appear to be three factors that have combined to bring about the strand cleavage between residues D-17 and G-18 at the Pb(1) site. If any one of these conditions was lacking, the strand cleavage would most likely not occur. These conditions are as follows: (1) The pK_1 value of a Pb(II)-bound water molecule has a value near 7 (that is, physiological pH), which will facilitate the reaction at pH 7.4 and slow it substantially at pH 5.0. The Pb(II) ion that is bound to one region of the folded tRNA molecule acts, as it were, as a local metalloenzyme and cleaves another section of the chain that passes nearby. (2) A Pb(II)-bound hydroxyl group must be in the correct orientation and at the correct distance from the 2′-OH group which it is to activate via the proposed proton abstraction. (3) The $tRNA^{Phe}$ molecule in both the native and derivative structures has large temperature factors for residues D-16 and D-17, which indicates that this section of the molecule is more flexible than the rest: if strand cleavage occurs by reaction of an activated 2′-OH with an adjacent phosphate P atom, then that reaction will be more facile in flexible regions of the molecule than in stacked double-helical regions.

Lack of Cleavage at Sites Pb(2) and Pb(3). The fact that cleavage is not observed at sites Pb(2) and Pb(3), at least not after short incubations with Pb(II) since this metal ion will eventually degrade the complete molecule given sufficient time, is not due to the absence of suitable Pb···tRNA contacts at these sites (Table II).

At site Pb(2) (Figure 4c) the electrophilic activation mechanism is unlikely to cause cleavage since the shortest Pb(2)···O(phosphate) distance is 4.1 Å to OL(A-44). Direct attack on P by a Pb(II)-bound hydroxyl group would seem to be a possibility since there is a Pb(2)···P(A-44) = 5.5 Å distance. All other such distances at this site are greater than 6.1 Å. The Pb(2)···O2′(A-21) = 6.7 Å distance is a little longer than the optimal distance of 6.0 Å for proton abstraction at 2′-OH to occur. The proton of O2′(A-21) may be involved in two hydrogen-bonding interactions with OL(G-22) at 2.7 Å or O6(m^7G-46) at 2.8 Å (Jack et al., 1976). All other Pb(2)···O2′(ribose) distances are greater than 8.3 Å.

At site Pb(3) (Figure 4d), the Pb(3)···OL(A-36) = 5.4 Å contact is the shortest such distance, and the electrophilic activation mechanism can therefore be ruled out as can direct attack on P by a $(Pb–OH)^+$ moiety since Pb(3)···P(A-36) = 6.2 Å is the shortest such distance at this site. As far as abstraction of H^+ from 2′-OH goes, the Pb(3)···O2′(Cm-32) = 6.2 Å distance would not lead to cleavage since the O2′ is methylated in this particular nucleotide. The Pb(3)···O2′(U-33) = 6.2 Å distance is a good candidate for strand scission via this mechanism. Since cleavage is not observed here, it is likely that one or more of the three necessary conditions required for cleavage via this mechanism, that were mentioned above, are lacking. There is a possible hydrogen bond between the proton of O2′(U-33) and N7(A-35) where the distance between these two atoms is 2.9 Å (Jack et al., 1976). It is noteworthy, however, that in some other species of tRNA cleavage is observed in this region of the anticodon loop (Werner et al., 1976).

Catalytic Nature of the Cleavage Reaction. In many instances the term "metal ion promotion" is a more rigorous description of the role played by a metal ion in a particular reaction since the metal is consumed stoichiometrically in that reaction (Bender, 1963). In the present work, however, we believe that the term "metal ion catalysis" may indeed be appropriate and that this is supported by our crystallographic experiments.

The Pb(II) ion occupancy at site Pb(1) in the structure at pH 7.4 is about 50% of that observed for the uncleaved structure at pH 5.0 (Table I, Figure 2). This implies that a certain percentage of the $tRNA^{Phe}$ molecules in the crystals at pH 7.4 have Pb(II) ions bound and, presumably, strand cleavage has not yet occurred. This is consistent with the 50% cleavage found in the biochemical experiments under similar conditions. Within other molecules in the crystals, the lower occupancy at this pH suggests that after strand cleavage has occurred the Pb(II) ion involved in that cleavage is released from the macromolecule and, theoretically at least, is free to bind to and cleave other $tRNA^{Phe}$ molecules. This means that the cleavage reaction would be catalytic and not stoichiometric.

We have therefore sought biochemical corroboration of the crystallographic results, which suggest that the cleavage reaction at residues D-17–G-18 is catalytic. Experiments were performed wherein varying concentrations of Pb(II) were added to a solution of 20 μM $tRNA^{Phe}$ under crystallizing conditions at pH 7.4 and after varying times the reaction

products were run on polyacrylamide gels.

At a concentration of 10 μM Pb(II), that is, a Pb:tRNA ratio of 1:2, about 75% of the tRNA molecules are cleaved in 238 h (data not shown). Had the reaction been stoichiometric in the sense defined above, the cleavage would not have exceeded 50%. Indeed, it should also be remembered that there are three lead binding sites, of about equal strength, so that only one-third of the Pb(II) ions are free, at least initially, to take part in the cleavage at site Pb(1).

The lowest concentration of Pb(II) we have used was 5 μM, corresponding to a Pb:tRNA ratio of 1:4, and here cleavage to the extent of about 10% was observed after 48 h. So if there is a threshold concentration to the Pb(II) cleavage, it must be below 5 μM. If the reaction is left to proceed longer than 3 weeks, more than one-fourth of the tRNA molecules were cleaved, again pointing to a catalytic reaction.

These reactions are slow, no doubt because the experiments were carried out in the presence of a large excess of Mg(II), which will compete with the Pb(II) for the binding sites. We therefore increased the concentrations of tRNA and $Pb(OAc)_2$ by a factor of 10, keeping the Mg(II) concentration the same. At 50 μM Pb(II) and 200 μM tRNA, i.e., a ratio of 1:4, we found at room temperature 33% cleavage after 2 days, 50% after 1 week, and 66% after 2 weeks. There is little doubt that the reaction is catalytic as defined above.

Apparent Sequence Specificity. A study of the Pb(II)-sensitive sites in several tRNA species demonstrates that there is a clear preference for cleavage after pyrimidines, especially modified uridine residues such as dihydrouridine (Werner et al., 1976). There appears to be no simple chemical explanation for the apparent sequence specificity of cleavage by Pb(II). Cleavage sites are found in the single-stranded D and anticodon loop regions at locations where, by analogy with tRNA^{Phe}, sharp bends might be expected to occur in the secondary structure. It is possible that the local conformation of the phosphodiester chain in these cases is also stereochemically favorable for chain scission at these sites. In yeast tRNA^{Phe}, residues D-17–G-18 are an example of a bend similar in structure to those formed by U-33–Gm-34 and Ψ-55–C-56. It is not surprising that D-17 participates in a bend in view of its poor base-stacking properties. It is significant that bends are closely associated with the four strongly bound Mg(II) ions in tRNA^{Phe}. In fact, the Pb(II) ion that induces the cleavage between D-17–G-18 replaces Mg(II) at one of these sites.

An unusual C2′-*endo*-ribose and the poor base-stacking properties of dihydrouridine confer a nonhelical conformation upon residue D-17. The absence of a hydrogen bond between the 2′-OH of ribose-17 and the oxygen O1′ of ribose-18 may, therefore, facilitate the interaction of the 2′-OH group with the Pb(II) ion. The involvement of a 2′-OH group in the cleavage mechanism is somewhat more hindered in stacked regions and may explain why the anticodon loop in tRNA^{Phe} is less susceptible to Pb(II) cleavage.

Reaction Pathway: Adjacent vs. In-Line. We have presented evidence above to suggest that the most likely mechanism for the Pb(II)-catalyzed cleavage of tRNA^{Phe} at site Pb(1) is by deprotonation of the 2′-OH of ribose-17 followed by nucleophilic attack of the resulting 2′-O$^-$ on the phosphorus atom of phosphate-18 (Figure 8). Our end group analyses indicate that the products of this cleavage reaction are a cyclic 2′,3′-phosphate at ribose-17 and a 5′-OH at G-18. Such cyclic 2′,3′-phosphates have also been identified, in other studies, as reaction products in the Pb(II)- and Zn(II)-promoted degradations of RNA at or near neutral pH (Dimroth et al., 1959; Britten, 1962; Huff et al., 1964; Butzow & Eichhorn, 1971). It is well established that acid- and base-catalyzed hydrolysis of RNA proceeds via a pentacoordinate phosphorus cyclic intermediate to yield, after chain scission, a cyclic 2′,3′-phosphate and a 5′-OH (Brown & Todd, 1952; Brown et al., 1956). We propose, therefore, that the cleavage at site Pb(1) also proceeds through a pentacoordinate phosphorus intermediate. Again, as discussed above, the first step in the generally accepted mechanism for RNase A (Roberts et al., 1969) is similar to that proposed by us for the cleavage at site Pb(1) with the $(Pb–OH)^+$ moiety activating the 2′-OH group, in the present case, whereas histidine-12 performs this function in RNase A. In both cases, the reaction is presumed to proceed via a trigonal bipyramidal (tbp) pentacoordinate phosphorus intermediate. It should be mentioned, however, that square-pyramidal intermediates may also be possible (Dewan & Kepert, 1975; Holmes, 1976, 1979; Holmes et al., 1978; Favas & Kepert, 1980).

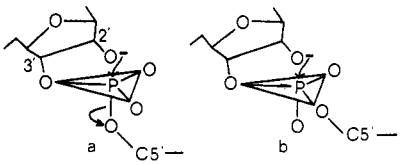

FIGURE 9: The (a) in-line and (b) adjacent mechanisms for attack of the 2′-O$^-$ group on the phosphate phosphorus atom. (a) The in-line mechanism where attack on phosphorus is opposite the leaving group, O5′, such that entering and leaving groups are in axial positions in the trigonal bipyramidal intermediate. (b) The adjacent mechanism where the entering group is axial but the leaving group is initially equatorial. A pseudorotation of the trigonal bipyramidal intermediate is necessary, to place the leaving group O5′ in an axial position, before bond scission can occur.

It was pointed out by Usher (1969) that all the mechanisms that had been proposed for RNase A at that time fell into two classes based on the geometry of the initial attack of the 2′-O$^-$ on phosphorus. If the attack on phosphorus is opposite the leaving group such that entering and leaving groups are in axial positions (also called apical positions) in the tbp, the displacement is called "in-line" (Figure 9a). If the entering group attacks phosphorus such that the leaving group is in an equatorial position (also called basal position), the displacement is called "adjacent", and a subsequent pseudorotation (Berry, 1960) of the tbp is required to place the leaving group in an axial position before bond scission can occur (Figure 9b). Both steps in the reaction of RNase A have been shown to proceed by the in-line pathway from the results of an elegant chemical (Usher et al., 1970, 1972) and structural study (Saenger et al., 1974).

Some of the statements in the previous two paragraphs derive from a set of five preference rules that are considered to apply to the reactions of model compounds that are related to RNA. One example is the hydrolysis of cyclic organophosphorus esters (Westheimer, 1968; Usher, 1969). The five rules are (1) hydrolysis proceeds by way of a pentacoordinate species that has the tbp geometry, (2) positional exchange can occur between the axial and equatorial positions of the tbp by means of a pseudorotation, (3) groups enter at and leave from axial positions only, (4) a five-membered ring (such as that formed by a ribose cyclic 2′,3′-phosphate) will span one axial and one equatorial position of the tbp, and (5) the more electropositive groups (such as –O$^-$) prefer equatorial positions, while the more electronegative groups (such as –O–R, where R is C3′ or C5′) prefer axial positions. As Usher (1969) has noted, the term "preference rules" is used to imply that processes that do not comply with the rules can occur but with a lower probability. Rule 3 derives from the principle of

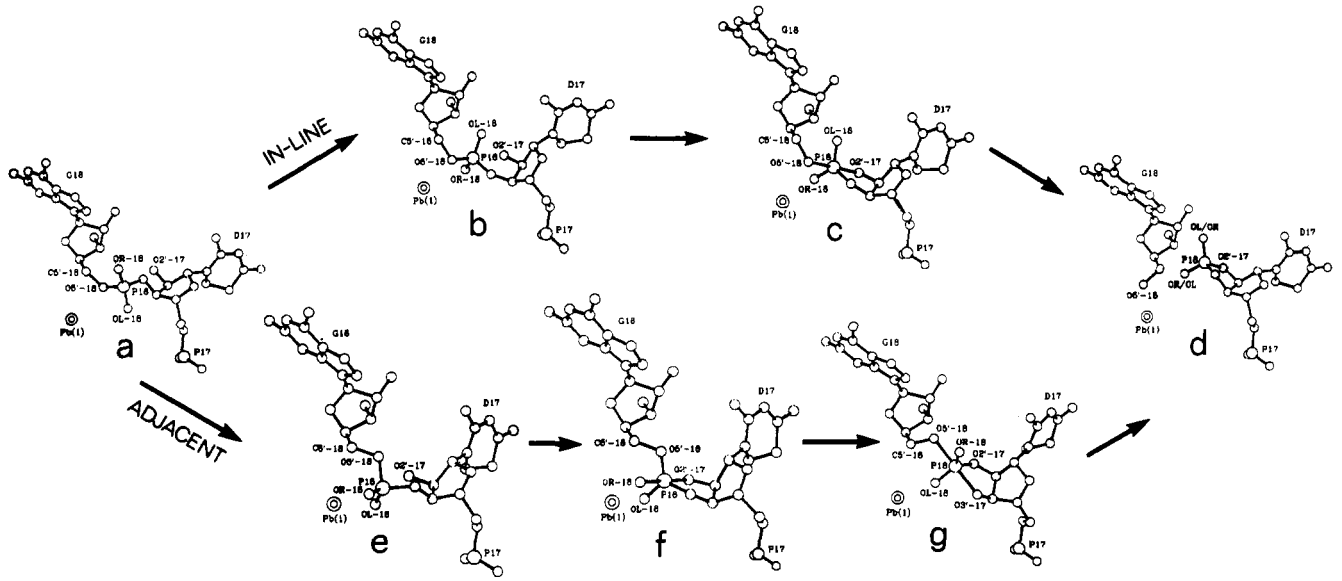

FIGURE 10: Possible in-line or adjacent pathways, as deduced from simple molecular models, for the strand scission between residues D-17 and G-18. (a) Native conformation. (b) After initial rotation of the sugar–phosphate backbone such that the O5′–P bond is set up for in-line attack by O2′. (c) Five-coordinate trigonal bipyramidal phosphorus intermediate. (d) The cyclic 2′,3′-phosphate product of the cleavage reaction. Note that the atom labeled OL/OR is OL for the in-line mechanism and OR for the adjacent mechanism. The opposite is true for the atom labeled OR/OL. (e) After initial rotation of the sugar–phosphate backbone such that the OR–P bond is set up for attack by O2′ in the adjacent pathway. (f) Five-coordinate trigonal bipyramidal phosphorus intermediate. (g) Five-coordinate intermediate after pseudorotation to place the O5′–P bond in an axial position prior to chain scission.

microscopic reversibility. Rule 4 is based on considerations of ring strain. For a bidentate ligand forming a five-membered ring, as is the situation in a ribose cyclic 2′,3′-phosphate, the O–P–O angle will be 90° when one oxygen atom is axial and the other equatorial whereas with both oxygen atoms equatorial the O–P–O angle is 120°, which is a highly strained situation for a five-membered ring. The situation with both oxygen atoms axial is obviously impossible. Rule 5 can be thought of in two ways (Gillespie, 1970). The first is that the smallest electron pairs, which have the smallest interactions with other electron pairs, tend to go to axial positions of the tbp (which are the more hindered sites) while larger electron pairs will occupy equatorial positions where there is more room for them. That is, the more electronegative ligands, which will have the smallest bonding electron pairs, always prefer axial positions. In our case, P–O^- is less electronegative than P–O–R (since $-O^-$ is saturated with electrons and will tend to give them up more readily than –O–R) and thus P–O^- will prefer equatorial while P–O–R will prefer axial positions in the tbp. An alternative way of looking at rule 5 is that in a tbp the equatorial bonds are shorter than the axial bonds. As such, the shorter terminal oxygen atoms in P–O^- groups will prefer equatorial positions while the longer P–O–R bonds, where the oxygen atom is bridging between two groups, will favor axial positions.

The crystal structure of $tRNA^{Phe}$ provides reasonably accurate atomic positions and geometry for the sugar–phosphate backbone and the Pb(1) atom, and we are therefore able to examine whether the cleavage reaction between D-17–G-18 might proceed via an adjacent or in-line pathway. For the arguments that follow we have assumed that there is a minimum of movement in the tRNA molecule in the region of the cleavage reaction at site Pb(1). Specifically this means that the bases and ribose rings of residues 17 and 18 remain in position during the reaction. This seems to be a fairly reasonable assumption since the crystallographic results at pH 7.4 (that is, after considerable strand cleavage has occurred) only show a negative peak at the position of phosphate-18 whereas if considerable movement of the tRNA molecule had occurred at this cleavage site we might have expected more extensive regions of significant negative electron density. Using simple molecular models, followed up on computer graphics facilities, we have been able to examine possible pathways for the cleavage reaction. A more quantitative study employing energy calculations is planned (B. E. Hingerty, personal communication) and calculations of that nature have already been performed on the RNase A reaction mechanism (Holmes et al., 1978; Allen, 1981). From our simple study it would appear that the adjacent mechanism is favored over the in-line mechanism since the initial conformation of $tRNA^{Phe}$ at the cleavage site (Figure 10a) seems such that the adjacent mechanism can occur with the least movement of the sugar–phosphate backbone. In fact, the tRNA conformation at residues 17 and 18 is very similar to that depicted in Figure 2 of the paper by Usher (1972), where it is pointed out that double-helical RNA should undergo chain scission via the adjacent pathway. In the present system the rotations required to bring phosphorus-18 close enough to the O2′ of ribose-17 are far less severe for the adjacent than they are for the in-line mechanism. The P18···O2′(ribose-17) distance in the native structure is 4.1 Å and must be reduced if a reaction is to occur between these two atoms. For consistency with our assumption that the nucleosides remain in place during the cleavage reaction, we assume that it is the phosphorus atom that moves toward O2′ and not vice versa. A similar assumption was made by Holmes et al. (1978) in their theoretical study of RNase A since, presumably, in binding to the active site of that enzyme the RNA is forced to adopt the relevant conformation.

For the *adjacent* mechanism there are two possible stereochemical pathways, and we label these *adjacent 1* and *adjacent 2*. The adjacent 1 pathway is the situation where O2′ enters the phosphorus coordination sphere opposite to OR while the adjacent-2 pathway is where O2′ enters opposite OL (Figure 10e). The rotations of the sugar–phosphate backbone for both of these adjacent pathways appear in Table SI, which is available as supplementary material (see paragraph at end of paper regarding supplementary material). Since adjacent-1 requires far less rotation of the sugar–phosphate backbone than

does adjacent-2, it is the most likely mechanism of the two, and we shall concentrate upon it here exclusively. Therefore, reference to the adjacent mechanism in this paper means adjacent-1 although most points of the discussion to follow will apply to both adjacent pathways.

We use the conformational nomenclature for the sugar–phosphate backbone that has been described by Sundaralingam (1973) and Jack et al. (1976), and the relationship between this and other conventions has been detailed by Berman (1981). For the adjacent mechanism (Figure 10) the major rotation of the sugar–phosphate backbone required to bring P18 close to O2′ of ribose-17 involves a change in the torsion angle ϕ' of ribose-17 by 90° from gauche$^+$ (272°) to a trans (182°) conformation. Changes in the other torsion angles are detailed in Table SI. Once reaction has occurred, O2′ and OR will be in the axial positions of the tbp (trigonal bipyramidal) intermediate, and for subsequent scission of the P–O5′ bond to occur, the tbp must undergo a pseudorotation such that O5′ and O2′ then occupy the axial positions of the tbp. For the in-line mechanism (Figure 10b), as well as the 132° rotation of the ϕ'_{17} torsion angle, further large rotations are necessary. These consist of a 97° rotation in the ω'_{18} torsion angle from gauche$^-$ (268°) to trans (171°) and of 104° in the ω_{18} angle from gauche$^-$ (245°) to trans (141°). Further smaller rotations are listed in Table SI.

It would appear, therefore, that from a consideration of rotations alone the adjacent mechanism requires far less movement of the sugar–phosphate chain than does the in-line mechanism. One factor that might favor the in-line mechanism, however, is that the rotations detailed above for the in-line case result in an unfavorable conformation of C3′–O3′–P18–O5′ where the ω' changes from an initial value of 268° to 171°. Such a *t,t* configuration for the ω',ω torsion angles of phosphate-18 is likely to be strained from a consideration of the calculations of Gorenstein et al. (1977a,b). Relief of this strain may be the driving force needed for the in-line mechanism to occur.

A complication of the adjacent reaction pathway is the requirement for protonation of oxygen OR (or OL) of phosphate-18 when occupying an axial position in the tbp. Subsequent deprotonation would force a pseudorotation to place the resulting P–O$^-$ in an equatorial position and place the O5′ leaving group in an axial position to allow strand scission. These events could only occur with the participation a second time of Pb(II)–OH$_2$ acting as a proton donor and then [Pb(II)–OH]$^+$ as a proton acceptor. That such an interaction is feasible is supported by the observation that in our model of the adjacent mechanism both OL and OR of phosphate-18 move closer to Pb(1) when adopting the conformations shown in Figure 10.

An advantage of the adjacent mechanism is that the reactants, the O2′ and O5′ oxygen atoms, are close together and thus require the action of a single general acid/base catalyst (Usher, 1969), in contrast to pancreatic ribonuclease where at least two histidine residues in the active site perform a similar function.

Molecular modeling by computer graphics of the possible reaction pathways also provides an explanation of the large negative peak in the difference Fourier map (Figure 2a) at the position of phosphate-18. Cleavage produces a ribose cyclic 2′,3′-phosphate, and formation of a bond between O2′ of ribose-17 and the phosphorus atom of P-18 moves the latter atom 2.9 Å from its original position in the native structure. However, as discussed above, the crystallographic data were collected before the cleavage was complete, so that although the loss of phosphate shows, its movement through intermediate stages will be smeared in the electron density maps.

Implications: Lead Toxicity and RNA Hydrolysis. The question of lead toxicity and the manner in which lead exerts its toxicity is not a simple one (Gilfillan, 1965; Vallee & Ulmer, 1972; Eisinger, 1978; Williams & Halstead, 1982; Royal Commision on Environmental Pollution, 1983). It is generally believed that metals such as Pb(II) and Hg(II) are toxic since they will preferentially bind to protein sulfhydryl groups, thereby inactivating the protein involved. Recent examples exist where this mode of lead toxicity may be operative (Farkas & Stanawitz, 1979; Blair et al., 1982). Since Pb(II) is so effective at cleaving RNA near physiological pH of ca. 7.4, it is highly likely that this is also a possible mechanism for the toxicity of this metal, and in one example, at least, Pb(II) was found to be extremely efficient at inhibiting haemoglobin synthesis in vitro in rabbit reticulocytes (Borsook et al., [illegible]7). The study of lead chemistry itself has not been popula[illegible] ... recent years, and the last study of the effect of Pb(II) upon RNA was carried out some 10 years ago. There are signs, however, of a renewed interest in the ability of Pb(II) to cleave RNA and in the strong possibility that this may be one way in which lead exerts its toxic effect (Harrison et al., 1983; Harrison & Healy, 1983; P. G. Harrison, personal communication).

One problem with the idea that Pb(II) cleavage of RNA is one reason for the toxicity of lead is that in vivo there is a high concentration of glutathione within the cell and this compound may bind and thus deactivate Pb(II) ions. Experiments concerning this point are to be encouraged. There may also be other metal scavengers present such as metallothioneins. Nevertheless, the free Pb(II) concentration in blood can be as high as 1.5 μM (Annest et al., 1983), and this concentration is of the order of that at which we have observed "catalytic" cleavage, even in the presence of competing ions.

In our preliminary account of the work presented here (Brown et al., 1983), we suggested that metal ions may be involved in the phenomenon of self-splicing RNA or the "ribozyme" (Zaug et al., 1983). An elegant mechanism involving two Mg(II) ions has now been proposed for the series of chain scissions and ligations that are known to occur in that system (L. C. Allen, personal communication). It has also been discovered recently that the catalytic activity of the enzyme ribonuclease P is carried out by RNA and not by protein (Guerrier-Takada et al., 1983). This system requires a high Mg(II) concentration, and there is little doubt that this metal ion plays a crucial chemical role in this process. One would expect that the RNA possesses a binding site for a well-positioned metal ion directed toward the scissile bond in the substrate, in a similar manner to that found here in the Pb(II)–tRNA system. Also, self-cleavage of a precursor RNA from bacteriophage T4 has recently been reported, and this cleavage requires at least a monovalent cation (Watson et al., 1984).

Another interesting area of related research involves that of prebiotic synthesis where metal ions such as Zn(II) and Pb(II) have been found to catalyze the synthesis of oligoribonucleotides (Lohrmann et al., 1980; van Roode & Orgel, 1980). Little information is available concerning the mechanisms of these reactions, but they could presumably occur by the reverse of the mechanism proposed in this work for the cleavage of tRNA^{Phe}.

ACKNOWLEDGMENTS

We thank B. E. Hingerty, S. E. V. Phillips, A. Mondragon, D. Rhodes, D. A. Usher, A. R. Fersht, D. M. Brown, P. G.

Harrison, O. W. Howarth, C. Carlson, and P. Riedinger for advice and help of various kinds.

Supplementary Material Available

Table SI listing the torsion angles for the proposed intermediates depicted in Figure 10 (1 page). Ordering information is given on any current masthead page.

Registry No. Pb, 7439-92-1.

References

Ahrland, S., Chatt, J., & Davies, N. R. (1958) *Q. Rev., Chem. Soc. 12*, 265.

Allen, L. C. (1981) *Ann. N.Y. Acad. Sci. 367*, 383.

Annest, J. L., Pirkle, J. L., Makuc, D., Neese, J. W., Bayse, D. D., & Kovar, M. G. (1983) *N. Engl. J. Med. 308*, 1373.

Arnone, A., Bier, C. J., Cotton, F. A., Day, V. W., Hazen, E. E., Richardson, D. C., Richardson, J. S., & Yonath, A. (1971) *J. Biol. Chem. 246*, 2302.

Baes, C. F., & Mesmer, R. E. (1976) *The Hydrolysis of Cations*, pp 358–365, Wiley, New York.

Bamann, E., Trapmann, H., & Fischler, F. (1954) *Biochem. Z. 326*, 89.

Barrell, B. G. (1971) in *Procedures in Nucleic Acid Research* (Cartoni, G. L., & Davies, D. R., Eds.) Vol. 2, pp 751–779, Harper and Row, New York.

Bender, M. L. (1963) *Adv. Chem. Ser. No. 37*, 19.

Berman, H. M. (1981) in *Topics in Nucleic Acid Structure* (Neidle, S., Ed.) Vol. 1, pp 1–15, Macmillan, London.

Berry, R. S. (1960) *J. Chem. Phys. 32*, 933.

Beveridge, K. A., & Bushnell, G. W. (1979) *Can. J. Chem. 57*, 2498.

Blair, J. A., Hilburn, M. E., Leeming, R. J., McIntosh, M. J., & Moore, M. R. (1982) *Lancet*, 964.

Borsook, H., Fischer, E. H., & Keighley, G. (1957) *J. Biol. Chem. 229*, 1059.

Britten, R. (1962) *C. R. Trav. Lab. Carlsberg 32*, 371.

Brown, D. M. (1974) in *Basic Principles in Nucleic Acid Chemistry* (T'so, P. O. P., Ed.) Vol. 2, pp 38–44, Academic Press, New York.

Brown, D. M., & Todd, A. R. (1952) *J. Chem. Soc.*, 52.

Brown, D. M., Magrath, D. I., Neilson, A. H., & Todd, A. R. (1956) *Nature (London) 177*, 1124.

Brown, R. S., Hingerty, B. E., Dewan, J. C., & Klug, A. (1983) *Nature (London) 303*, 543.

Buckingham, D. A. (1977) in *Biological Aspects of Inorganic Chemistry* (Addison, A. W., Cullen, W. R., Dolphin, D., & James, B. R., Eds.) pp 141–196, Wiley, New York.

Burgess, J. (1978) *Metal Ions in Solution*, pp 264–267, Horwood, Chichester, U.K.

Butzow, J. J., & Eichhorn, G. L. (1965) *Biopolymers 3*, 95.

Butzow, J. J., & Eichhorn, G. L. (1971) *Biochemistry 10*, 2019.

Butzow, J. J., & Eichhorn, G. L. (1975) *Nature (London) 254*, 358.

Carrabine, J. A., & Sundaralingam, M. (1971) *Biochemistry 10*, 292.

Cingi, M. B., Manfredotti, A. G., Guastini, C., & Nardelli, M. (1972) *Gazz. Chim. Ital. 102*, 1034.

Cingi, M. B., Manfredotti, A. G., Guastini, C., & Musatti, A (1975) *Gazz. Chim. Ital. 105*, 117.

Cotton, F. A., Bier, C. J., Day, V. W., Hazen, E. E., & Larsen, S. (1971) *Cold Spring Harbor Symp. Quant. Biol. 36*, 243.

Cotton, F. A., Hazen, E. E., & Legg, M. J. (1979) *Proc. Natl. Acad. Sci. U.S.A. 76*, 2551.

Dewan, J. C., & Kepert, D. L. (1975) *J. Chem. Soc., Dalton Trans.*, 959.

Dimroth, K., & Witzel, H. (1959) *Justus Liebigs Ann. Chem. 620*, 109.

Dimroth, K., Jaenicke, L., & Heinzel, D. (1950) *Justus Liebigs Ann. Chem. 566*, 206.

Dimroth, K., Witzel, H., Hulsen, W., & Mirbach, H. (1959) *Justus Liebigs Ann. Chem. 620*, 94.

Drew, M. G. B., & Nelson, S. M. (1979) *Acta Crystallogr., Sect. B: Struct. Crystallogr. Cryst. Chem. B35*, 1594.

Drew, M. G. B., Rodgers, A., McCann, M., & Nelson, S. M. (1978) *J. Chem. Soc., Chem. Commun.*, 415.

Drew, M. G. B., Cabral, J. deO., Cabral, M. F., Esho, F. S., & Nelson, S. M. (1979) *J. Chem. Soc., Chem. Commun.*, 1033.

Eichhorn, G. L. (1975) in *Inorganic Biochemistry* (Eichhorn, G. L., Ed.) Vols. 1 and 2, pp 1232–1235, Elsevier, New York.

Eichhorn, G. L., & Butzow, J. J. (1965) *Biopolymers 3*, 79.

Eichhorn, G. L., Butzow, J. J., Clark, P., & Tarien, E. (1967) *Biopolymers 5*, 283.

Eichhorn, G. L., Tarien, E., & Butzow, J. J. (1971) *Biochemistry 10*, 2014.

Eisinger, J. (1978) *Q. Rev. Biophys. 11*, 439.

England, T. E., Bruce, A. G., & Uhlenbeck, O. C. (1980) *Methods Enzymol. 65*, 65.

Farkas, W. R. (1968) *Biochim. Biophys. Acta 155*, 401.

Farkas, W. R. (1975) *Chem.-Biol. Interact. 11*, 253.

Farkas, W. R., & Stanawitz, T. (1979) *J. Inorg. Biochem. 11*, 31.

Farkas, W. R., Hewins, S., & Welch, J. W. (1972) *Chem.-Biol. Interact. 5*, 191.

Favas, M. C., & Kepert, D. L. (1980) *Prog. Inorg. Chem. 27*, 325.

Fersht, A. R. (1977) *Enzyme Structure and Mechanism*, pp 49–51, W. H. Freeman, San Francisco.

Gilfillan, S. C. (1965) *J. Occup. Med. 7*, 53.

Gillespie, R. J. (1970) *J. Chem. Educ. 47*, 18.

Gorenstein, D. G., Findlay, J. B., Luxon, B. A., & Kar, D. (1977a) *J. Am. Chem. Soc. 99*, 3473.

Gorenstein, D. G., Luxon, B. A., & Findlay, J. B. (1977b) *J. Am. Chem. Soc. 99*, 8048.

Groves, J. T., & Dias, R. M. (1979) *J. Am. Chem. Soc. 101*, 1033.

Guerrier-Takada, C., Gardiner, K., Marsh, T., Pace, N., & Altman, S. (1983) *Cell (Cambridge, Mass.) 35*, 849.

Harrison, P. G. (1976) *Coord. Chem. Rev. 20*, 1.

Harrison, P. G., & Steel, A. T. (1982) *J. Organomet. Chem. 239*, 105.

Harrison, P. G., & Healy, M. A. (1983) *Inorg. Chim. Acta 80*, 279.

Harrison, P. G., Healy, M. A., & Steel, A. T. (1982) *Inorg. Chim. Acta 67*, L15.

Harrison, P. G., Healy, M. A., & Steel, A. T. (1983) *J. Chem. Soc., Dalton Trans.*, 1845.

Hingerty, B., Brown, R. S., & Jack, A. (1978) *J. Mol. Biol. 124*, 523.

Hingerty, B. E., Brown, R. S., & Jack, A. (1980) in *Biomolecular Structure, Conformation, Function and Evolution* (Srinivasan, R., Ed.) Vol. 1, pp 293–302, Pergamon Press, Oxford.

Hingerty, B. E., Brown, R. S., & Klug, A. (1982) *Biochim. Biophys. Acta 697*, 78.

Hodgson, D. J. (1977) *Prog. Inorg. Chem. 23*, 211.

Holbrook, S. R., Sussman, J. L., Warrant, R. W., Church, G. M., & Kim, S. H. (1977) *Nucleic Acids Res. 4*, 2811.
Holmes, R. R. (1976) *Int. J. Pept. Protein Res. 8*, 445.
Holmes, R. R. (1979) *Acc. Chem. Res. 12*, 257.
Holmes, R. R., Deiters, J. A., & Galluchi, J. C. (1978) *J. Am. Chem. Soc. 100*, 7393.
Houttemane, C., Boivin, J. C., Thomas, D. J., Canonne, J., & Nowogrocki, G. (1981) *Acta Crystallogr., Sect. B: Struct. Crystallogr. Cryst. Chem. B37*, 686.
Huff, J. W., Sastry, K. S., Gordon, M. P., & Wacker, W. E. C. (1964) *Biochemistry 3*, 501.
Jack, A., & Levitt, M. (1978) *Acta Crystallogr., Sect. A: Cryst. Phys., Diffr., Theor. Gen. Crystallogr. A34*, 931.
Jack, A., Ladner, J. E., & Klug, A. (1976) *J. Mol. Biol. 108*, 619.
Jack, A., Ladner, J. E., Rhodes, D., Brown, R. S., & Klug, A. (1977) *J. Mol. Biol. 111*, 315.
Kepert, D. L. (1970) *Proc. R. Aust. Chem. Inst. 37*, 135.
Kon, A. Yu., & Bourshteyn, I. F. (1976) *Kristallokhim. Neorg. Soedin*, 150.
Ladner, J. E., Finch, J. T., Klug, A., & Clark, B. F. C. (1972) *J. Mol. Biol. 72*, 99.
Ladner, J. E., Jack, A., Robertus, J. D., Brown, R. S., Rhodes, D., Clark, B. F. C., & Klug, A. (1975) *Proc. Natl. Acad. Sci. U.S.A. 72*, 4414.
Lerner, E. I., & Lippard, S. J. (1977) *Inorg. Chem. 16*, 1537.
Lohrmann, R., Bridson, P. K., & Orgel, L. E. (1980) *Science (Washington, D.C.) 208*, 1464.
Markham, R., & Smith, J. D. (1952) *Biochem. J. 52*, 552.
Marzilli, L. G., Kistenmacher, T. J., & Eichhorn, G. L. (1980) in *Metal Ions in Biology* (Spiro, T. G., Ed.) Vol. 1, pp 180–250, Wiley, New York.
Nishimura, S. (1972) *Prog. Nucleic Acid Res. Mol. Biol. 12*, 49.
North, A. C. T., Phillips, D. C., & Matthews, F. S. (1968) *Acta Crystallogr., Sect. A: Cryst. Phys., Diffr., Theor. Gen. Crystallogr. A24*, 351.
Pearson, R. G. (1963) *J. Am. Chem. Soc. 85*, 3533.
Pierce-Butler, M. A. (1982) *Acta Crystallogr., Sect. B: Struct. Crystallogr. Cryst. Chem. B38*, 2681.
RajBhandary, U. L., Stuart, A., Hoskinson, R. M., & Khorana, H. G. (1968) *J. Biol. Chem. 243*, 565.
Roberts, G. C. K., Dennis, E. A., Meadows, D. H., Cohen, J. S., & Jardetzky, O. (1969) *Proc. Natl. Acad. Sci. U.S.A. 62*, 1151.
Robertus, J. D., Ladner, J. E., Finch, J. T., Rhodes, D., Brown, R. S., Clark, B. F. C., & Klug A. (1974) *Nature (London) 250*, 546.
Royal Commission on Environmental Pollution (1983) *Lead in the Environment*, Ninth Report, Cmnd. 8852, HMSO, London.
Rubin, J. R., & Sundaralingam, M. (1983) *J. Biomol. Struct. Dyn. 1*, 639.
Saenger, W., Suck, D., & Eckstein, F. (1974) *Eur. J. Biochem. 46*, 559.
Silberklang, M., Prochiantz, A., Haenni, A. L., & RajBhandary, U. L. (1977) *Eur. J. Biochem. 72*, 465.
Silberklang, M., Gillum, A. M., & RajBhandary, U. L. (1979) *Methods Enzymol. 59*, 58.
Sundaralingam, M. (1973) in *Jerusalem Symposia on Quantum Chemistry and Biochemistry* (Bergmann, E. D., & Pullman, B., Eds.) Vol. 5, pp 417–455, Israel Academy of Sciences, Jerusalem, Israel.
Swaminathan, V., & Sundaralingam, M. (1979) *CRC Crit. Rev. Biochem. 6*, 245.
Sylva, R. N., & Brown, P. L. (1980) *J. Chem. Soc., Dalton Trans.*, 1577.
Trapmann, H., & Devani, M. (1965) *Hoppe-Seyler's Z. Physiol. Chem. 340*, 81.
Usher, D. A. (1969) *Proc. Natl. Acad. Sci. U.S.A. 62*, 661.
Usher, D. A. (1972) *Nature (London), New Biol. 235*, 207.
Usher, D. A., Richardson, D. I., & Eckstein, F. (1970) *Nature (London) 228*, 663.
Usher, D. A., Erenrich, E. S., & Eckstein, F. (1972) *Proc. Natl. Acad. Sci. U.S.A. 69*, 115.
Vallee, B. L., & Ulmer, D. D. (1972) *Annu. Rev. Biochem. 41*, 91.
van Roode, J. H. G., & Orgel, L. E. (1980) *J. Mol. Biol. 144*, 579.
Vijayan, M., & Viswamitra, M. A. (1966) *Acta Crystallogr. 21*, 522.
Walker, R. T., & RajBhandary, U. L. (1975) *Nucleic Acids Res. 2*, 61.
Watson, N., Gurevitz, M., Ford, J., & Apirion, D. (1984) *J. Mol. Biol. 172*, 301.
Werner, C., Krebs, B., Keith, G., & Dirheimer, G. (1976) *Biochim. Biophys. Acta 432*, 161.
Westheimer, F. H. (1968) *Acc. Chem. Res. 1*, 70.
White, A. H., & Willis, A. C. (1977) *J. Chem. Soc., Dalton Trans.*, 1362.
Williams, D. R., & Halstead, B. W. (1982) *J. Toxicol., Clin. Toxicol. 19*, 1081.
Wintermeyer, W., & Zachau, H. G. (1973) *Biochim. Biophys. Acta 299*, 82.
Witzel, H. (1959) *Justus Liebigs Ann. Chem. 620*, 122.
Wlodawer, A., Miller, M., & Sjolin, L. (1983) *Proc. Natl. Acad. Sci. U.S.A. 80*, 3628.
Woolley, P. (1975) *Nature (London) 258*, 677.
Yu, M. W., & Fritchie, C. J. (1975) *J. Chem. Soc., Dalton Trans.*, 377.
Zaug, A. J., Grabowski, P. J., & Cech, T. R. (1983) *Nature (London) 301*, 578.